

Bond graphs in modeling plant water dynamics

by
Julia Miersch

A thesis submitted to the
Faculty of
Electrical and Computer Engineering
University of Arizona, Tucson

In partial fulfillment of the requirements for the degree of
Diplom-Ingenieurin
Fachrichtung Maschinenbau
Universität Stuttgart
1996

**The University of Arizona
Graduate College**

I hereby approve the following report prepared under my direction at the
University of Arizona:

Bond graphs in modeling plant water dynamics

accomplished by

Julia Miersch

Thesis Director

Professor Dr. Francois Cellier
Department of Electrical and Computer
Engineering

Date

Contents

1	Bond graphs	9
2	water potential and phenomena of water	13
3	Transportation and water storage in plants	18
3.1	Water uptake by roots	18
3.2	Water uptake in the vessels of the shoot system	21
3.3	Water pathway in the leaf and transpiration	23
3.4	the stomata	24
4	measurement of water status	29
5	the hydraulic flow model	33
6	bond graph of the hydraulic architecture of agave	37
7	The energy balance of a plant	43

7.1	net radiation	45
7.1.1	Estimation of average solar radiation	46
7.1.2	long-wave radiation	47
7.2	sensible and latent heat flow between atmosphere-plant	49
7.3	Implementation of the energy balance in Dymola	52
7.4	The Penman-Monteith equation	57
A	plots	67
B	programs	72
B.1	program:agave.dym	72
B.2	program bond.lib	77
B.3	agave.dec	81
B.4	program:agave.dyc	82
B.5	program:veg.dym	84
B.6	program:veg.lib	87
B.7	program:veg.dec	93
B.8	program:veg.dyc	96

List of Figures

1.1	passive circuit	11
1.2	bond graph for a passive circuit	12
1.3	bond graph for a passive circuit ready for implementation in Dymola	12
2.1	bondgraph for diffusion through a membrane	17
3.1	root in cross section	19
3.2	longitudinal section through part of a vascular bundle in a stem	21
3.3	resistances of the leaf	24
3.4	transverse section of a leaf	25
3.5	stomatal responses	27
5.1	bond graph of a simplified plant	36
6.1	bond graph of an agave	38
6.2	bond graph of tissues hydraulic architecture	39

7.1	bond graph for the energy balance of a plant	44
7.2	bond graph for the energy balance of a plant under steady state conditions .	45
7.3	simulation run for a capacity of $4.19e5kJ/K$	56
A.1	waterflow into and out of storage	68
A.2	transpiration and uptake by the root	68
A.3	water potential	69
A.4	difference in wateruptake for the outer chlorenchyma between simulations run with constant and variable osmotic pressure	69
A.5	transpiration rate and osmotic potential	70
A.6	water flow out of storage	71
A.7	water potential	71

Acknowledgments

I would like to express my deepest gratitude to Dr. Francois Cellier, my advisor, for his guidance and encouragement throughout this study.

I am very grateful to Dr. Rocco Fazzolari and Dr. Alfred Voss for making the exchange program between the University of Arizona and the University of Stuttgart possible.

Special Thanks also to Roland Krueger at the IER in Stuttgart, who took care of all the formalities before and during my stay.

Furthermore, I would like to thank Biosphere2 for the valuable insight obtained during my internship.

Abstract

Objective of this research was to apply the bond graph representation to models describing plant processes. Two models that deal with the water dynamics of vegetation were chosen. One describes the water dynamics within the plant, called the hydraulic flow model, the other describes the energy fluxes into and out of the system plant.

The hydraulic flow model is a mechanistic model used to study the movement and storage of water in different plant organs as well as overall water movement through the plant. It was put into bond graph notation and applied to a study by [15] of an agave. The energy balance of a plant considers the energy fluxes into and out of heat and metabolic storage. In ecology it is used to analyze the relations between net radiation, latent and sensible heat flux. A bond graph for this purpose is developed and implemented in Dymola, using models found in ecology for the description of radiation input, stomatal and boundary layer conductance of heat and mass transfer.

Introduction

Bond graphs give a representation of a system that, keep the topological structure and provide a computational structure. They can be used for simulations in object-oriented languages such as Dymola, in which the code is easily read and modified. Further their topological structure provides important information about a system. Bond graphs show between which system components power is exchanged and how subsystems are influenced by incoming or outgoing power fluxes and signals. Aim of this research was to investigate their application to modeling vegetation.

Bond graph notations of plant processes are able to describe and simulate systems such as the Biosphere2, where technology and nature are coupled. Technology defines atmospheric conditions in the Biosphere2, causing vegetation to produce changes in system variables such as humidity and CO_2 concentration, which again can be altered with technical help. Bond graphs have been used in biomedical and biochemical models, however only few projects have used them to model plants or plant communities. R.R. Allen [1] developed a conceptual model of the CO_2 uptake by a leaf, the photosynthetic process and the translocation of photosynthetic material to other plant parts. G.H. Smerage [23] showed the possibility of describing a plant with bond graphs, but without determining the parameters or equations describing the system.

Therefore the first step was a literary research in plant physiological and ecological modeling. It proved, that many models found could not be used for bond graph notation, since they were exclusively based on mass-balances and did not consider, the power flows connected to the process under observation. There is a reason for it. The degree of complexity of phenomena in biology often make the derivation of a physical model extremely difficult or impossible. Instead empirical relations are used to describe system responses. Two models found, that could be represented with bond graphs were the hydraulic flow model and the energy balance. Both are used to study water dynamics. The hydraulic flow model deals

with water dynamics within the plant. It assigns capacitances and resistances to water flow in different plant parts. The energy balance simplifies greatly the structure of a plant to a layer of common properties, which do not change over space. It is used to determine evaporation rate or water dynamics between vegetation and atmosphere. It describes the energy fluxes into the thermal storage of the plant.

The first chapter of this report will give an introduction to bond graphs. Chapter two introduces the driving force in the hydraulic flow model, the water potential, and will look at some properties of water that are held responsible for water movement in plants. The following three chapters will look at the transport of water in a plant, the hydraulic flow model and a bond graph notation thereof. To create a bond graph of a system the following questions have to be answered: What variables will be used as effort and flow? Where and what are the major compartments between which power flows? Which elements or subsystems will describe the observed system sufficiently? The flow through the different plant parts and how they are modeled is discussed in chapter three. Chapter four reviews measuring techniques of water related variables, since they are crucial to parameterization. Chapter five and six discuss the hydraulic flow model and an apply it to an agave.

The energy balance is introduced in chapter seven. Common models in ecology for the description of the different energy fluxes are reviewed and used in an implementation of the energy balance in Dymola.

Chapter 1

Bond graphs

Bond graphs are a graphical representation technique, that considers the energy flow between subsystems of a process, phenomenon or system under observation. Bond graphs are a means of representing the computational structure of a system without losing knowledge of its topological structure. They are best explained, when deriving them for electrical systems, but they can be applied to a variety of other physical, chemical and biological systems. Bond graphs work with junctions, elements and nodes. Bonds pass on two variables from node to node or node to element. These two variables are called effort and flow, or across and through variable respectively. In electrical circuits the effort is the potential or potential difference and the flow is the current. Table 1 summarizes effort and flow for different physical systems.

The product of effort and flow of each bond equals the energy flux from one subsystem to the next connected by the bond. In other words the bond stands for the power transmitted from one compartment to the next.

	effort	flow
electrical	voltage	current
translational	force	velocity
rotational	torque	angular velocity
hydraulic	pressure	volume flow
chemical	chemical potential	molar flow
thermodynamical	temperature	entropy flow

Table1

Two genders of junctions exist: zero and one. The zero junction describes Kirchhoff's node law. The one junction describes the mesh law. For electrical systems the main elements are resistance, capacitance and inductance, voltage and current sources. If a system includes several physical systems, for example mechanical and electrical, transforming elements are used, describing the transformation of one effort into another, e.g. from force into voltage etc.

Elements contain equations describing the subsystem they represent. Together with the laws connected to the nodes a set of equations for the system under observation can be derived. During this process several rules have to be considered. To derive the computational structure of a system a causality needs to be applied to the bond graph representation. Each bond is involved in two equations, one to determine the effort, one to determine its flow. A stroke perpendicular to the bond arrow indicates at which of the two nodes connected by the bond the flow is calculated. Only one flow can be calculated at a 0-junctions. Only one flow can be calculated away from a 1-junction. The flow is determined at a flow source and away from an effort source. It is determined at an inductor and away from a capacitor. If alternatives in assigning causalities exist, the system contains algebraic loops. If it is impossible to assign correct causalities the system is structurally singular.

Bond graphs can be implemented in the object-oriented simulation language Dymola.

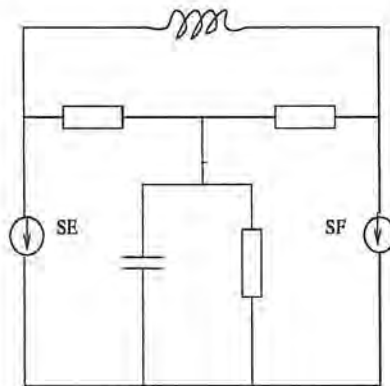


Figure 1.1: passive circuit

There are additional rules to implementing bond graphs in Dymola. Elements are always attached to 0-nodes. Node genders toggle between each other.

Figure 1.1 shows a passive circuit. The bond graph is derived by introducing 0-nodes for nodes of common potential and 1-nodes for elements over which the potential changes. The ground node was omitted, because the bonds connecting it to the system represent zero transmitted power. Elements are connected to 1-nodes and nodes are connected by bonds according to the flows and assumed flow directions. Figure 1.2 shows the bond graph derived in that manner. It can be simplified by omitting the structure bond-node-bond that has only one flow going in and out of a node into one bond. For the implementation in Dymola elements have to be connected to 0-nodes and node genders have to toggle between one another leading to the bond graph shown in Figure 1.3.

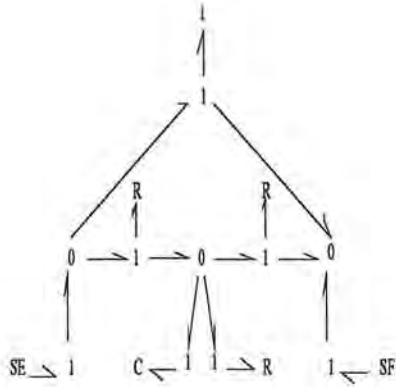


Figure 1.2: bond graph for a passive circuit

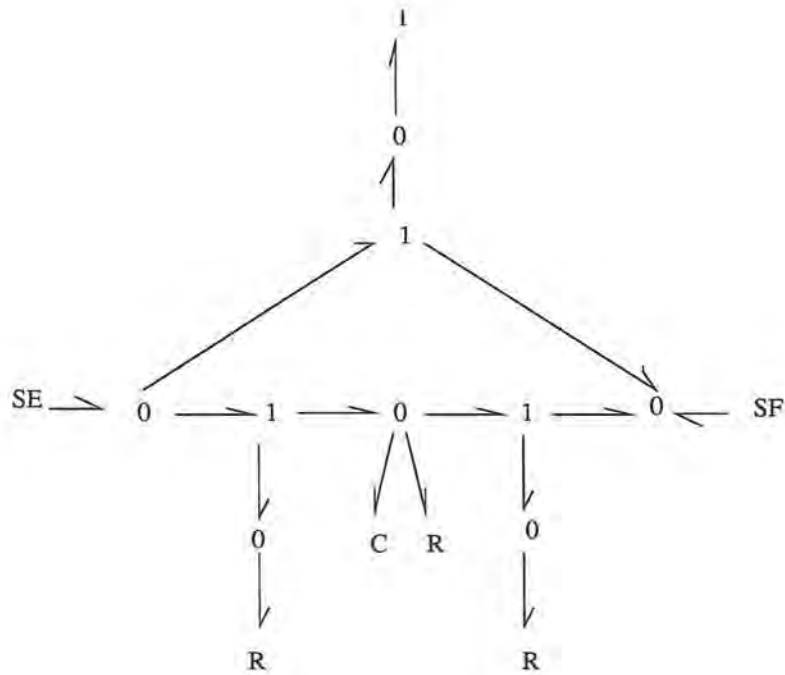


Figure 1.3: bond graph for a passive circuit ready for implementation in Dymola

Chapter 2

water potential and phenomena of water

Before looking at water transport, storage and the different mechanisms presumably responsible for water dynamics within a plant, one should look at an important value in plant water status, the water potential and at the general properties of water. The properties of water cause a variety of phenomena, that are involved in plant processes. Water potential will be the effort source in the hydraulic flow model.

water potential

Water potential is the most commonly used measure of water status in plants. It indicates how much free energy is available to do work, e.g. to induce sap flow in the vessels of the stem or move water from the soil to the root via diffusion. Water potential is defined as the sum of chemical, hydrostatic, electrical, and gravitational potential divided by the molar

volume of water.

$$(\Psi - \Psi_0) * \bar{V}_w = R * T * \ln a_j + \bar{V}_w * P + z_j * F * e + m * g * h \quad (2.1)$$

Since in pure water or very dilute solutions the electrical ($z_j * F * e$) part is zero, so it can be omitted. In describing physical systems potential differences and not absolute values are of importance and therefore the reference potential Ψ_0 is arbitrarily set to zero. The water potential is said to have osmotic, hydrostatic and gravitational parts. Hydrostatic potential difference plays the dominant part in transportation up the xylem vessels while water uptake from the soil to the roots can be driven by a difference in water concentration hence the osmotic potential difference.

$$\Psi = \Psi_{\Pi} + \Psi_P + \Psi_g \quad (2.2)$$

Hydrostatic pressure Ψ_P

Due to the rigid cell walls of plants it is possible to develop pressures above atmosphere. The hydrostatic pressure difference between the environment and the cell is called turgor pressure. A plant will wilt at zero turgor. Hydrostatic pressure differences within the plant are believed to cause sap flow up tall trees. As water evaporates it sets the water column in the vessels under tension inducing a flow. The magnitude of this tension or pressure difference along the shoot depends on the difference of evaporation and water uptake by the roots. The reason for the water in the vessels being under tension, instead of a breaking of the water column lies in its properties. Water molecules form hydrogen bonds. They giving rise to adhesive forces, which act between a solid and water, and cohesive forces, that exist between water molecules. Phenomena such as capillary rise and surface tension can be explained with help of these forces. Capillary rise and cohesion are the most accepted causes for rise of sap in plants.

Osmotic pressure Ψ_{Π} and Gravitation Ψ_g

Osmosis is the net flow of water crossing a differentially permeable membrane separating two solutions of differing solute concentration. It is driven by the concentration difference. Osmotic pressure is defined as the pressure that needs to be applied to prevent water flow from a region of lower to a region of higher concentration. Osmotic potential of a species is defined as the negative of the osmotic pressure. It can be determined for an ideal solution with Van't Hoff's law. Dilute solutions have properties very similar to ideal solutions and can also be estimated by it.

$$\Psi_{\Pi} = -R * T * c_s \quad (2.3)$$

Van't Hoff's law relates changes in water potential to changes in concentration times the absolute temperature and the ideal gas constant. Gravitation has to be considered in the movement of water up tall trees. The gravitational potential increases with 1 bar/ 10 m height, it is defined as $\Psi_g = \rho * g * h$

water characteristics

The attributes of water are made responsible for many phenomena in plant processes. The adhesive and cohesive forces of water, e.g. are seen as two of the causes for the ascent of sap. The following sections will only give an overview for water characteristics that are important to the transportation process.

Hydrogen bonds

Hydrogen bonds are strong intermolecular forces resulting from the structure of H_2O . The oxygen atom is strongly electro-negative and tends to draw electrons away from the hydrogen atoms. The positively charged hydrogens are electro-statically attracted to the

negatively charged oxygen of two neighboring water molecules causing hydrogen bonding. Hydrogen bonds cause forces between surfaces and water (adhesive) and forces within bulk water (cohesive).

capillary rise

If a capillary is held into a liquid, the strong adhesion of water molecules to a wettable wall will cause the fluid in a capillary to rise. Due to the cohesive force in the bulk solution, water is continually pulled up the capillary as water rises along its walls. The water will stop to rise the moment the adhesive force and the gravitational force of the water column have come to an equilibrium.

surface tension

Surface tension can be seen as the force that needs to be exerted to expand the water surface by unit area. It is the energy that is needed to break the hydrogen bonds that are lost in moving water molecules from the interior to the surface. Surface tension considerably adds to soil resistance, because in addition to adhesive forces in soil cavities air-water surfaces will form in unsaturated soil.

Diffusion

Diffusion is the movement of molecules of a species from a place of lower concentration to a point of higher concentration. The assumption of one dimensional diffusion is sufficient for most transport processes within plants. It is described by Fick's law of diffusion. Fick's law is an empirical approach, that states that the mass flow of a species is proportional to the concentration difference, the species density, a diffusion coefficient and inversely proportional

to the distance. A common phenomena in biology is the diffusion over a semi-permeable membrane. The movement of water and solutes into or out of cells and organelles is characterized by diffusion over several membranes. This is called osmosis. The driving force for the diffusion can be seen as the difference in chemical potential or as the difference in concentration. Diffusion can be represented in bond graph presentation as by [10]:

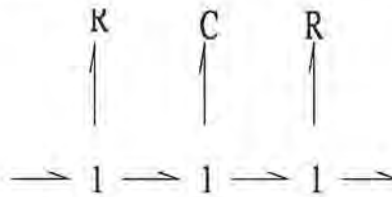


Figure 2.1: bondgraph for diffusion through a membrane

Chapter 3

Transportation and water storage in plants

Water is taken up in radial direction to the root cylinder driven by a difference in water potential between root and soil. It diffuses into the central cylinder of the roots where the vessels are, that connect water flow from the root up the stem to the leaves. As water at the top of the column diffuses from the vessels into the cells of the leaf and from there into the pores of the stomata, it moves upward due to the cohesive and adhesive forces of water. In the pores it evaporates and transpires through the stomatal openings into the atmosphere. The two most important mechanisms making the transport of water possible in a plant are diffusion and a pressure gradient within the vessels inducing a hydraulic flow.

3.1 Water uptake by roots

Root hairs of absorbing roots grow in the cavities of the soil, from where they obtain water and ions solved in it. Water transport from the soil into the vessels of the central cylinder of the root holding the xylem vessels is driven by a difference in water potential. Absorption

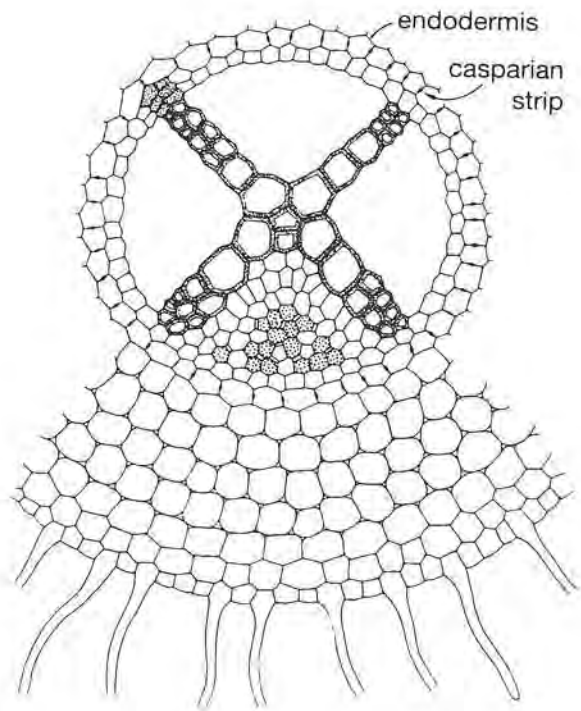


Figure 3.1: root in cross section

is split into active or osmotic-driven uptake and passive or transpiration driven uptake. Active absorption is dominant in slowly transpiring plants, while passive absorption occurs in rapidly transpiring plants. Passive absorption often lags behind transpiration, indicating the existence of resistances to water flow and water storage in the different organs. A drop in water potential through transpiration is transmitted from the leaves via the vessels to the roots inducing a flow into the roots up the stem. The accumulation of salts in the central cylinder of the root leads to a concentration difference between root and soil, causing osmotic-driven water uptake. This osmotic pressure is called root pressure. It exists only under good environmental conditions in healthy roots. Influencing factors are the composition of soil solvents, mild temperatures and well aerated roots.

Factors influencing water uptake by the root

Using an approach analogous to Ohm's law to model water flow through an organ or otherwise chosen subsystem of the soil-plant-atmosphere continuum, water flow (\dot{V}) can be described as the water potential difference over a certain compartment ($\Delta\Psi$) divided by its resistance (R_c).

$$\dot{V} = \Delta\Psi/R_c \quad (3.1)$$

Factors changing water uptake will either be expressed in a change of the water potential difference or a change in resistance. Hence water potential and resistance can be functions of time, temperature, nutrients supply, etc. Soil water potential decreases during dehydration of soil. Soil resistance increases with dehydration. As the soil dries its bigger pores and capillaries dry out first. Remaining water in small capillaries and pores is bound by stronger adhesive forces and surface tension, requiring more work to extract it. Soil-root-surface resistance increases due to soil and root shrinking, that reduces root-soil surface contact. Drying soil causes additional buildup of suberin, a wax-like substance increasing root resistance. Low temperature and deficient aeration leads to a decrease in conduction of membranes as well as an increase in the viscosity of water, increasing the root's resistance.

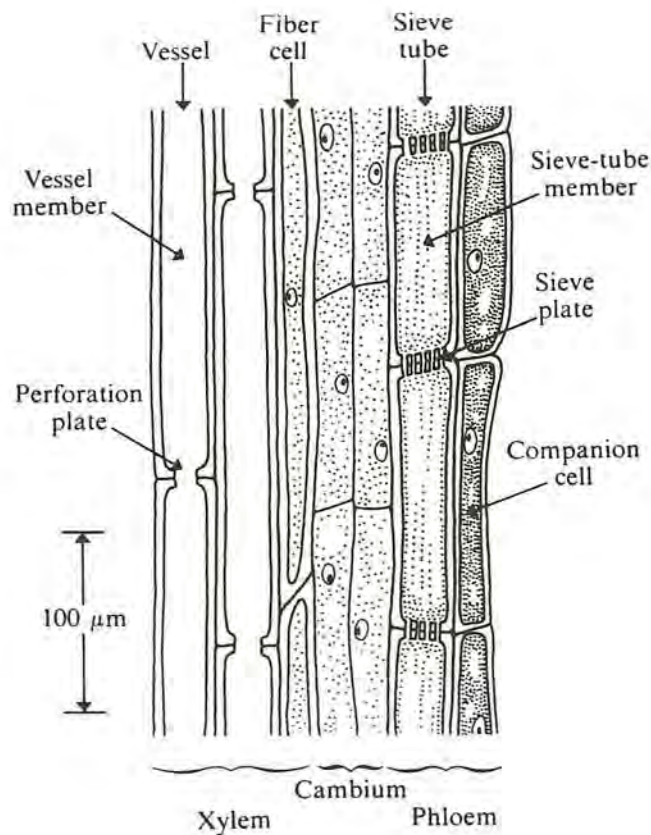


Figure 3.2: longitudinal section through part of a vascular bundle in a stem

3.2 Water uptake in the vessels of the shoot system

Long-distance transport of water in plants takes place in the xylem of vascular bundles. Two basic vessel elements exist for plants, vessel members and tracheids. In plants with tracheids the cross walls of cells forming the vessel partly dissolve during maturation forming long capillary tubes. The vessel decreases in diameter on both ends. They are connected to each other by bordered pits, which are a substantial resistance to sap flow. Tracheids are common in conifers. Vessel members tend to be shorter and wider than tracheids, with a more constant diameter. In vessel members cells lose their protoplasts. The remaining cell walls form a pathway for sap. Vessel members are in series to one another, divided

by perforation plates forming long tubes with a low flow resistance. Their length is in the magnitude of centimeters to meters. They are found in angiosperms. Water rise in the vessels may have several mechanisms superposed. All can be traced back to the distinctive properties of water explained earlier and the structure of wood. The small diameters of xylem and the holes in the perforation plates of vessels cause considerable capillary rise. The most excepted theory of sap rise in plants is the cohesion tension theory. It postulates that cohesive forces sustain a water column despite transpiration by the leaves, putting the water column in the vessel under tension as long as water uptake lags behind transpiration and pulling water up the stem. Vessels are under suction or negative pressure for most of the time, reaching maximum tension when water uptake lags most behind transpiration. Vessels react only slightly elastically to those forces, but enough to cause a change in tree trunk diameter. The flow in the vessels can be described approximately by Hagen-Poiseuille's law for laminar flow in a tube.

$$\frac{\partial V}{\partial t} = -n \frac{\pi R^4}{8\eta_0} \frac{\partial P}{\partial z} \quad (3.2)$$

$\frac{\partial P}{\partial z}$ is the difference in pressure potential across a tissue segment of a length of ∂z , holding n vessels with a mean radius of R , η is the viscosity of water. Approximating the flow through vessel members with the Hagen-Poiseuille formula is more adequate for vessel members than tracheids. The bordering pits in coniferous trees add considerably to hydraulic resistance requiring a modification of [Hagen-Poiseuille]. The analytical derivation of hydraulic resistance requires a considerable amount of information. It is error prone even for angiosperms, because in many cases the structure of wood is only poorly described as conducting tubes in parallel, requiring the modification of results by correcting factors. For practical purpose hydraulic flow in the shoot vessels can be described with help of the Darcy's equation. In Darcy's equation the difference in hydrostatic pressure equals the volume flow times the resistance.

$$\Delta P = QR \quad (3.3)$$

R then can be determined as the ratio of change in pressure over extracted sap per time interval of a stem segment in the pressure bomb.

Capacitance effects

As water potential is lowered in the conducting vessels and transpiration increases, water will move not only laterally but also radially into the vessels under tension. On the other hand water will move from the vessels into dehydrated tissues as the plant equilibrates with its environment at night (with the exception of CAM plants that transpire at night). As a result the water content of the tissue changes. The capacitance of a tissue is defined as the change in the amount of water content to the change in water potential:

$$C = \frac{dW}{d\Phi} \quad (3.4)$$

The specific capacity of the tissue can be determined from the Hoeffler Diagram, described in Chapter 4.

3.3 Water pathway in the leaf and transpiration

Water diffuses from the vessels into the leaf mesophyll cells and evaporates from the mesophyll cell walls or the inner side of leaf epidermal cells through the inter-cellular airspaces to the stomata and then into the outside air. The pathway of water through a leaf can be described in a network analogy as by Nobel in [9], see Figure 3.3. The water can evaporate at the air water-interfaces of mesophyll cells or the inner side of epidermal cells in a leaf before diffusing into the pathways of the inter-cellular air spaces. Water generally has to cross a thin waxy layer on the cell walls within a leaf. After crossing this waxy layer, the water vapor diffuses through the inter-cellular air spaces and then through the stomata to reach the boundary layer adjacent to the leaf surface. Alternatively, the water in the cell walls

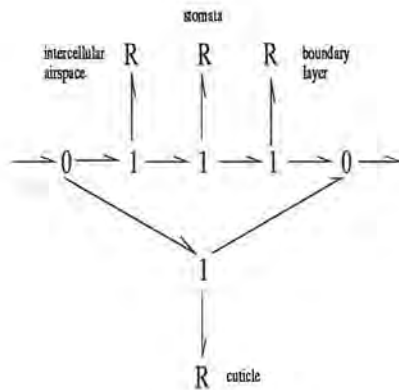


Figure 3.3: resistances of the leaf

might move as a liquid to the cell walls on the cuticular side of the epidermal cells, where it could evaporate and diffuse across the cuticle (or water can move as a liquid across the cuticle) before reaching the boundary layer [9]. This pathway has a very high resistance due to the thick wax like cuticle and therefore is often neglected when modeling transpiration.

3.4 the stomata

Functionally, stomata may be regarded as hydraulic valves. A relative rise of turgor pressure in the guard cells causes the pores to open. Stomata close when the difference in turgor between guard and neighboring cells diminish. Usually, stomatal guard cells are accompanied by two relatively large neighboring cells, called subsidiary cells, with which they form the stomatal apparatus. The subsidiary cells possess a storage function for ions and H_2O and form an elastic anchor point for the guard cells. In all stomatal complexes the opening movement is triggered by a decrease of water potential in the guard cells relative to their neighboring cells. This causes a passive influx of water and thus a rise of turgor. The decrease in Ψ can be traced to a corresponding increase in osmotic potential, under the influence of light, low atmospheric CO_2 concentrations, temperature etc. Conversely signals inducing closure, e.g. the hormone ABA that is emitted when roots experience water stress,

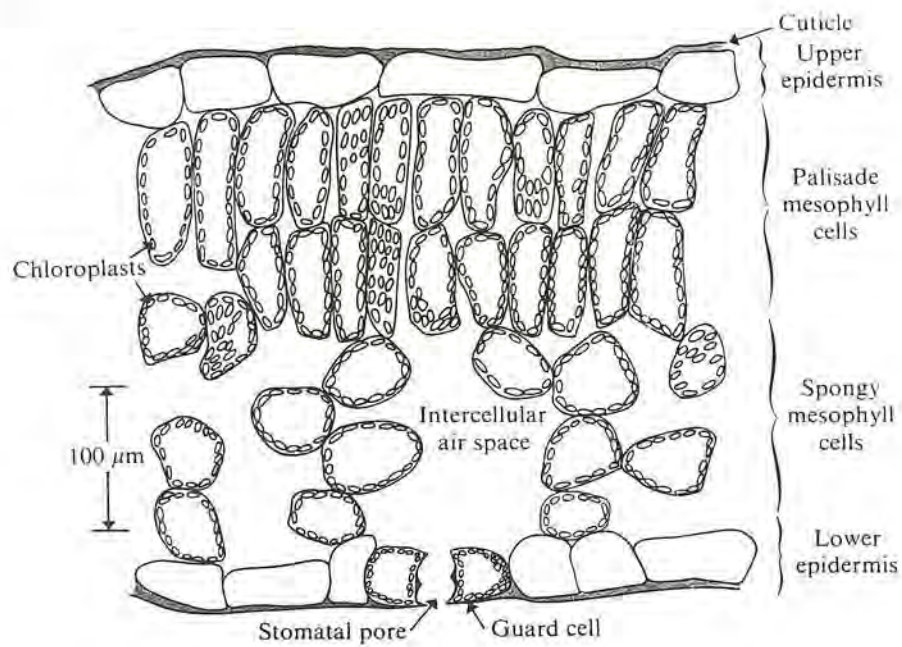


Figure 3.4: transverse section of a leaf

lead to a decrease in osmotic potential (or increase in water potential) and thus to the efflux of water from the guard cells. In the regulation of the stomata ions play a decisive role in increasing osmotic potential. In more than fifty species rapid transport of K^+ between neighboring and guard cells has been shown. The control of this ion-transport in guard cells is so far only partly understood. Thus, when modeling stomatal behavior, known responses to environmental factors are considered, e.g. light, temperature, atmospheric and intercellular CO_2 concentration etc.. [20].

models for stomatal resistance

Stomatal functioning is determined by many factors and therefore describing the behavior of the plant's most important control instrument is arbitrarily difficult.

Figure 3.5 shows functions modeling stomatal response taken from [6]. Figure 3.5A shows the relation to incoming photonflux, figure 3.5B to water-vapor deficit in the atmosphere, Figure 3.5C to atmospheric temperature and Figure 3.5D shows the response to changes in leaf water potential. The following section introduces two approaches to modeling stomatal conductance as a function of different environmental factors. They are used to model the stomatal control of large vegetation covers. Their validity for single plants and smaller biomes e.g. greenhouses has to be investigated.

Stomatal resistance according to Taconet et al[1986]

$$r_s = r_0 \frac{800(1 + 0.5LAI)}{(1 + S)LAI} \quad (3.5)$$

The stomatal conductance model as suggested by Taconet is proportional to the LAI, incoming short wave radiation and a constant depending on season and vegetation type.

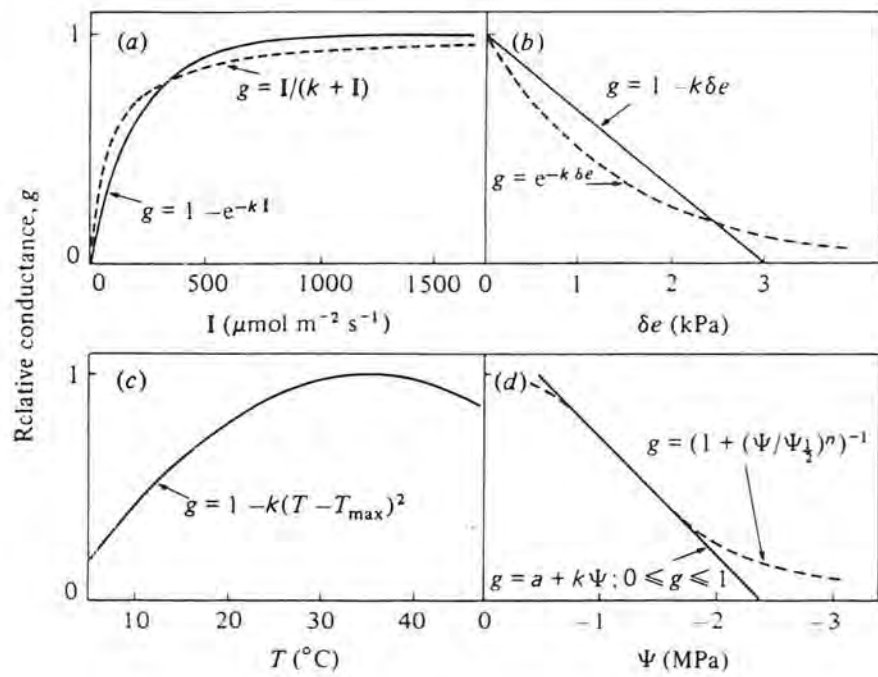


Figure 3.5: stomatal responses

Stomatal resistance according to Ball-Berry

This photosynthetic conductance model takes the net assimilation rate A_n , the relative humidity h_s and the partial pressure c_s of CO_2 at leaf surface as influencing variables and calculates stomatal conductance as follows:

$$g_s = m \frac{A_n}{c_s} h_s p + b \quad (3.6)$$

m and b are vegetation-type specific parameters. Net assimilation rate equals the assimilation plus the respiration rate. The calculations of the control variables and their determining factors are described in [13].

boundary layer resistances to heat and mass transfer of leaves

The heat conductance at plant-surface-atmosphere is a function of wind speed and surface characteristics. Conductance found on leaves has been found close to engineering values derived for flat horizontal plates. A β factor is used to describe derivations. Usually β is between 1 and 2.5. Monteith and Unsworth [19] suggest that the additional heat loss, which is especially noticeable under laminar conditions is caused by a rather unstable boundary layer, which must exist on a narrow leaf with irregular edges and curved profile. Hairs improve heat conduction additionally. Similarly, comparisons have been made for the conductance of mass transfer. Jones suggest a multiplication with the factor of 1.5. He further advises that it is best, to determine the boundary layer resistance empirically by measuring it from wet surfaces of same shape under the same conditions.

Chapter 4

measurement of water status

There are several objectives for measuring plant water status. One aim is to measure sap flow and potential differences between two locations to later determine resistances and capacitances describing the water dynamics of the plant segment by empirical relations. Capacitances and resistances to water flow can also be determined with help of anatomical features.

On the other hand, measurements of water potentials are simply taken as an indicator of plant water stress. A common problem with taking measurements of water relevant variables is that the methods are mostly destructive. This limits the acquirable data, which is crucial to the parameterizations of continuous models.

measurement of soil water potential

Measurement of soil water potential is critical. Soil potential depends on grain and pore size and water content. Soil is a very inhomogeneous material and therefore potential may vary considerably over space. Total soil water potential can be measured by burying thermocouple psychrometers protected by enclosure in porous or stainless steel screen cylinders at various depths. An alternative is to sample soil and analyze it in the lab. In a psychrometer tissue or, in this case, soil is allowed to come to water vapor equilibrium with air in a small chamber, the humidity of which is previously known. The result can be calibrated against known water potentials of solutions. Osmotic potentials of extracted sap can be measured the same way or by using a osmometer which measures freezing point depression. Another way to determine soil potential is to measure soil water content and use empirical formulas relating them for different soils as in [21].

Determination of leaf water potential

Leaf water potential is usually determined with the pressure bomb or a psychrometer. A pressure bomb or chamber is a destructive measure. A leaf or twig is sealed in a chamber with its cut end in contact with the atmosphere. The chamber is then pressurized until sap starts flowing out of the cut end. The pressure used to extract the sap is equal to the leaf's or twig's water potential.

measurement of sap flow

Sap flow is either measured with the heat pulse method or with a constant heat source. A part of the stem is insulated, then exposed to the constant heat source at the beginning of the insulation. Further upstream, temperature is measured. The volume flow can then be

derived with help of the first law of thermodynamics as:

$$dV/dt = (T_{out} - T_{in})c_p/(\rho Q) \quad (4.1)$$

The volume flow is proportional to a difference in temperature between heat source and temperature measurements ($T_{out} - T_{in}$), to the specific heat capacity (c_p) of water divided by its density (ρ) and the heat flow it is exposed to. The heat pulse method has been replaced by the constant heat source and therefore is only mentioned here

measurement of xylem characteristics

The resistances to flow of a stem segment is determined by exposing the segment to a pressure difference over its length and measuring the extruded water over time. This is done in a pressure chamber. Measurements of hydrostatic pressure that dominate water potential in xylem are taken with the help of a pressure probe. The resistance is calculated with Darcy's law. A micro capillary is inserted into a vessel. The capillary is filled with a liquid that comes into contact with the xylem sap and therefore can transmit the xylem pressure to a pressure transducer. It is not certain how big of an error this method causes by disrupting at least part of the water column in the xylem.

measurements of tissue capacitance

Tissue capacitance is also determined with the pressure bomb. The tissue is systematically dehydrated by increasing applied pressure in steps. The extruded water is put in ratio to fully hydrated tissue water content. Capacitance is defined as the change in relative water content Θ to change in water potential Ψ or applied pressure. The relation between Ψ and Θ is displayed in Hoeffler-diagrams. Although in general non-linear, a constant value sufficiently approximates in many cases the tissue's behavior to water uptake.

transpiration rate

Transpiration is approximated with measurements of sap flow or with help of steady state-porometers. A branch is enclosed in a chamber through which air is pumped. Transpiration rate is determined with help of the flow velocity and the change in relative humidity between in and out flowing air.

Chapter 5

the hydraulic flow model

A model commonly used in plant physiology to study dynamics of water flow through vessels and water uptake by organ tissues is the hydraulic flow model. It uses Darcy's law to describe the resistance towards the flow through a plant be it on cellular pathways or along the xylem vessels. The hydraulic flow model takes into account the capacity for water uptake by the plant organs. The effort variable is the difference in water potential between two points, the flow is the volume flow of water. Ideally water potentials should only be compared between locations of same temperature. While neighboring compartments usually have the same temperatures, roots and leaves don't. Nevertheless, it is still a fair approximation for the driving force.

When studying the water dynamics of a plant, the compartments involved in it have to be defined. There are two basic pathways water can choose, cellular or via the vessels. Since these resistances are very different, it makes sense to distinguish between them. Further the plant can be divided into organs: the root, the shoot and the canopy etc.. Depending on the objective of a model the architecture of these compartments can be considered by introducing segments, as shoot branches for example, that work in parallel. Further organs can be split into several tissue layers, as done for the leaves of an agave in the example

given in the next chapter, if their behavior needs to be considered separately. Effort sources can model water potential differences imposed on the plant, as for example the difference between atmospheric and soil potential, or they can be used to describe the influence of the osmotic potential in a tissue layer on water dynamics.

Figure 5.1(A) shows a simplified tree. It consists of one root, a stem and a big leaf. Its hydraulic architecture can be described with bond graphs as seen in figure 5.1(B). This plant was partitioned into the following compartments: root, shoot and leaf. The compartment root includes one resistance. It describes the resistance water encounters on its path from the soil adjacent to the root through the root surface and root cortex ending in the xylem vessel of the root cylinder. This resistance will depend on soil water potential, nutrients, temperature, root age and health. For modeling purposes over a few days it can be assumed constant.

The compartment shoot is modeled with two flow resistances in the xylem in series (for simplicity's sake they include the resistance of the root xylem), which are in parallel to a storage resistor and capacitor. This part of the model describes the radial flow into storage tissue adjacent to the xylem and lateral flow in the xylem. Notice, that this is a lumped parameter model. A very small section of the xylem is modeled in the same manner. In this model a series of many of those very small sections are replaced with a model of equivalently larger resistances and capacitance.

The compartment leaf is modeled with a resistance to flow through the mesophyll cells, where water travels either trans-cellular or inter-cellular. An effort source models the change in water potential as water evaporates, presumably on the cell walls of the mesophyll cells into the inter-cellular airspaces. On its way to bulk air the water vapor will further encounter the resistance of the stomatal pores and the boundary layer. Stomatal resistance will vary with signals from the root, such as hormones as ABA, changes in water vapor or CO_2 differences between the bulk air and stomatal pores, leaf water potential, temperature, etc. All these influences could be modeled as signals making stomatal resistance highly nonlinear. The

resistance of the boundary layer depends on wind speed and surface characteristics.

The driving force is the difference in water potential between soil and atmosphere. Both are modeled as effort sources. In practice the leaf compartment is often replaced with a much simpler model, a total leaf resistance and a flow source: the transpiration rate, which can be easily measured. Substituting the model has several reasons. There are many known responses of stomatal conductance to environmental factors. Nevertheless the functioning of the stomatal apparatus is still not fully understood. Therefore, modeling stomatal conductance with help of known responses has its limitations. Another problem is the sensitivity of the effort source to changes in relative humidity. Fairly small changes in relative humidity cause big changes in water potential and therefore have great effect on the magnitude of the driving force of water flow within the plant, which is the water potential difference between soil and atmosphere, leading to big errors in calculation of the transpiration stream.

rel humidity	100.0	99.6	99.0	96.0	90.0	50.0	0.0
water potential	0.0	-0.54	-1.36	-5.51	-14.2	-93.6	$-\infty$

Unfortunately, this solution deprives the model of its ability to estimate transpirational flow. It still is a valuable tool to analyze water dynamics within the plant. The simplified model is shown in Figure 5.1(C).

Real plants have a complex architecture, with many resistances in parallel for each compartment. To determine the hydraulic flow resistance, one has to account for the branching and root structure and consider extra resistances at branching nodes as in [17]. This study takes into account the hydraulic architecture of a tree. The model characterizes the tree as a branched catena of 4000 stem segments. The hydraulic resistance of each segment is determined by its segment length, hydraulic conductance, which is a function of stem diameter and the number of branching nodes bordering the segment, leading to a considerable amount of effort in parameterization. After determining these parameters, they again can be aggregated to one for example characterizing total shoot behavior or total leaf resistance and capacitance as shown by the preceding chapter for an agave.

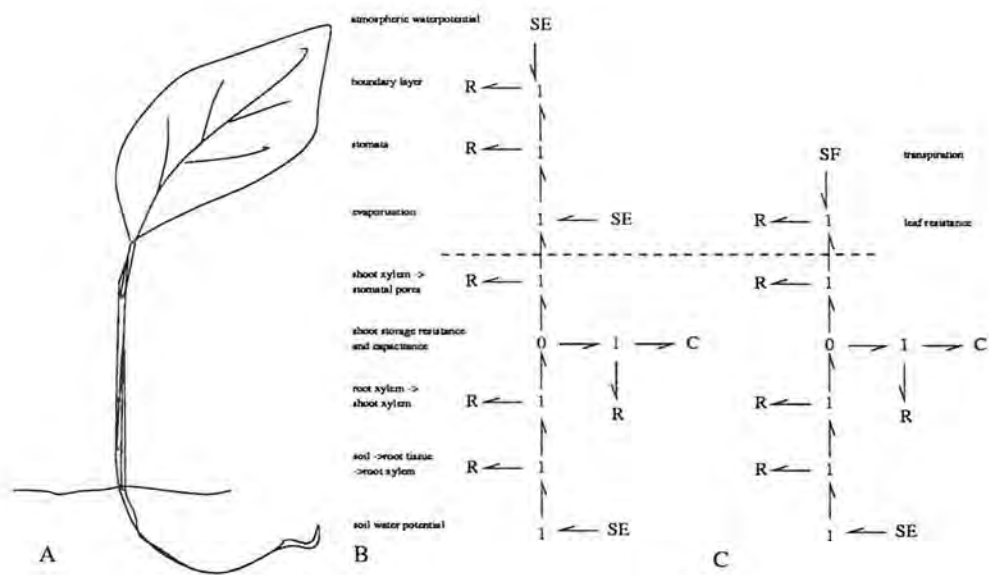


Figure 5.1: bond graph of a simplified plant

Chapter 6

bond graph of the hydraulic architecture of agave

In the study by [15] a hydraulic flow model for an agave was derived. Agave is a succulent plant. It grows in sparse-water environments. Its anatomy allows it to minimize evaporation. It exhibits low cuticular conductance and stomata density, forming a very high resistance to evaporation. Agaves have a high volume to surface ratio, allowing great water storage capacity. The agave shows crassulean active metabolism. CO_2 uptake and therefore transpiration occurs mainly at night, when the water-vapor pressure difference between outside and inside the stomata is lowest. The study's aim was to determine the influence of an increase in osmotic potential of the leaf tissue connected to CAM on transpiration with help of the hydraulic flow model.

The model's hydraulic architecture is grouped into roots, stem and three layers of leaf tissue: water storage parenchyma, inner chlorenchyma, outer chlorenchyma. The compartments of the tissues include the tissue layer of all leaves in parallel respectively. The leaves of the agave have been lumped into one big leaf by the model.

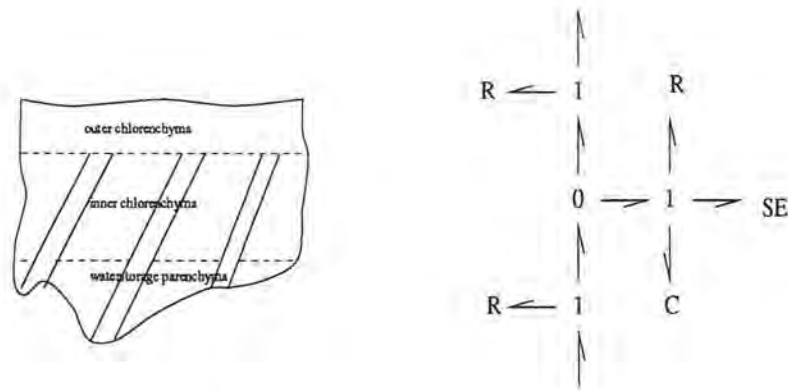


Figure 6.1: bond graph of an agave

Each of these compartments was assigned the same hydraulic architecture. It includes one resistance towards flow in the xylem in parallel with a resistance to flow in and out of storage and a capacity as well as an effort source. The effort source models osmotic behavior of the compartment and therefore its influence on the water potential of that compartment. Figure 6.1 shows an agave's leaf tissue and its structure: vessels penetrate the two inner layers water storage parenchyma and inner chlorenchyma, but end before reaching the outer chlorenchyma. On the right hand-side the hydraulic model for one tissue layer is displayed.

Water moves along the xylem to the outer layer, where it has to choose either the trans-cellular or inter-cellular pathway to the stomata.. In the xylem it not only moves laterally , but also radially out and into adjacent tissue depending on the difference in water potential between tissue and vessel. This process could be described as a chain of infinitesimally small xylem resistances in parallel to a storage uptake resistance and capacitor. The model is discretized over space in so far as it assigns two xylem resistances per tissue layer and one resistance and capacitor to describe uptake into the tissue.

It further considers osmotic potential of the tissue layer as a driving force and models it as an effort source. Osmotic potential increases during the night , because the CO_2 uptake causes an increase in acidity, that is reduced by photosynthesis during daytime. An increase in osmotic potential causes a decrease in waterpotential and attracts water to move into the

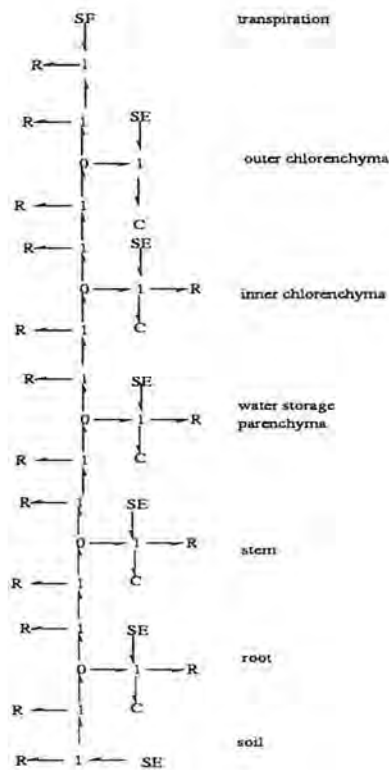


Figure 6.2: bond graph of tissues hydraulic architecture

tissue, therefore is a driving force. The potential difference at the capacitor represents cell turgor pressure according to the equation $\Phi = P + \pi$. P is the hydrostatic pressure and π is the osmotic potential, which is the negative of the osmotic pressure. Stem and root tissue are modeled the same way. Their values were determined by studies from [8]. Soil water potential was modeled as an effort source. Transpirational flow was modeled as a flow source. The use of a flow source as the driving force for water movement eliminates the need to consider stomatal resistances and changing leaf to air water potential differences, replacing these elements by the easily measured transpiration rate [15]. figure 6.2 shows the bond graph for the whole plant.

The plant analyzed had 27 leaves in parallel. Total xylem resistance for 27 leaves was calculated with a modified Hagen-Poiseuille for elliptic cross sections. Of this. 89 % was assigned to the water storage parenchyma and 11 % to the inner chlorenchyma. The resistance

of the outer layer of leaf tissue was calculated for a one-dimensional cellular pathway. The total leaf capacitance was partitioned according to the cell characteristics of the leaf tissues. Capacitances were measured with the pressure bomb as change in water volume over change in average water potential. Storage resistance was determined as the time for extrudation for a particular change in water content times the capacitance. Transpiration rate and cell osmotic potential were measured and used as inputs. The following table summarizes the values used for this simulation.

	units	root	stem	wsp	ich	och
storage resistance	[MPas/ m^3]	2.6e7	8.9e6	2.48e6	1.98e7	5.27e7
capacitance	[m^3 /MPa]	1.8e-5	1.8e-4	1.2e-3	2.19e-4	5.54e-5
xylem resistance	[MPas/ m^3]	6.2e5	2.88e6	1.56e6	1.96e5	-
osmotic pressure	[MPa]	0.67	0.67	var	var	var

For the implementation in Dymola xylem resistance of neighboring compartments were seen as one. Implementation was done with the dual bond graph avoiding otherwise necessary introductions of 0-nodes and additional bonds, so that elements can be connected to the 0-nodes. Simulation was done in time steps of 12-minutes, using a Runge-Kutta-fourth-order. Data was taken from study [15]. Dymola produced 22 coupled equations that were solved using a form of Cramer's rule for solving sets of algebraic equations by introducing auxiliary variables. It translated the solved equations into ACSL code, in which the experiment was run.

Programs `agave.dym`, `bond.lib`, `agave.dyc` and `agave.dec` are found in the appendix. `Agave.dym` contains the structure of the dual bondgraph found in 6.1 and the definition of the input and output values. `Bond.lib` is the standard bondgraph library containing models for flow and effort sources, inductances and conductances needed for the implementation of the agave's dual bondgraph. `Agave.dyc` is the command file. `Agave.dec` contains the tables with input information.

Simulations scenarios were carried out for measured osmotic pressure and osmotic pressure staying constant at its dusk values. Simulation was carried out for a 24-hour period starting shortly before dusk at 6pm for osmotic pressures as taken from the paper [15] and for osmotic pressures, which were lower by a factor of 1000.

Results similar to those found by [15], were only found when choosing osmotic pressures of a factor 1000 lower than those given in the paper. Simulation results were back-checked with help of Spice, which produced comparable results for a simulation run for the input values given by [15]. Using the values of osmotic pressures given in [15] led to a drop of water potential throughout the night and constant dehydration of the tissue layers. Simulation results with the osmotic pressures of a factor 1000 lower showed a drop of water potential during the night and an increase during daytime. Analogous, water flow out of the tissue occurred at night and tissues were recharged during day time.

Graph A.5 shows the measured transpiration rate and changing osmotic potential of the three leaf layers. These measurements are used as inputs for the simulation.

Graphs showing the organ's different responses are found in the appendix. Following graphs show the simulations with osmotic pressures of a factor 10^{-3} lower than those given in the paper [15]. Graph A.1 displays the flow of water into and out of storage for all five compartments. The greatest fluctuations are found in the water storage parenchyma and the outer chlorenchyma. The outer chlorenchyma has to compensate for sudden changes as transpiration accelerates shortly after dusk. The water flow out of the water storage parenchyma is more gradual, but lasts throughout the night. While outer chlorenchyma starts recharging early in the night water storage parenchyma provides water until early morning. The graph A.2 shows the measured transpiration rate and the uptake of water by the roots. According to this simulation with the low osmotic pressures water uptake is lower than transpiration and therefore the plant suffers dehydration. Figure A.3 displays the drop in water potential during the night. The biggest amplitude is observed in the outer chlorenchyma. There the change to increasing water potential occurs first, reflecting

the uptake of water into the tissue early during the night. As water potential drops water potential difference between xylem and tissue allows the tissue to be recharged, increasing water potential. Water storage parenchyma and inner chlorenchyma have a more gradual change of water potential, which turns positive during daytime. Turgor pressure strongly reflects changes in water potential according to $P = \Psi - \pi$. The differences in water uptake for the outer chlorenchyma and cell turgor between simulations runs for changing and constant osmotic pressures are displayed in figure A.4. It was the compartment where the difference was most evident. Still difference in water flow into or out of the tissue were in the range of 0.1% , indicating that osmotic potential has little effect in controlling transpiration. The differences in turgor pressure reflected exactly the difference in osmotic potential. The turgor pressures determined with constant osmotic pressure were lower than those with variable osmotic potential. Therefore a plant not showing the increase in osmotic potential of its leaves' tissues would wilt sooner.

Graph A.6 shows water flow into and out of the tissue layers for the simulation with the osmotic pressures given in the paper. Except for the outer chlorenchyma none of tissue layers is recharged. Water outflow from the parenchyma is approximately twice as large as water outflow in the simulation using the low osmotic pressure. Waterpotential is shown in the graph A.7. In the outer chlorenchyma it drops 36 times as much as the drop obtained from the simulation with lower osmotic values. Although the change in waterpotential turns positive during daytime, waterpotential has dropped in the outerchlorenchyma by 0.5 MPa by the end of the simulation day.

Chapter 7

The energy balance of a plant

The source in the hydraulic flow model was either modeled as the water potential difference between soil and air pulling water through the system or as a flow source: the transpiration rate. The transpiration rate can be determined with help of the energy balance, that can be put into bond graph notation as well. This requires the use of a different set of effort and flow. They are used to describe thermodynamic systems: temperature and entropy flux.

One way to describe plant processes is to look at the overall energy flows into and out of the system plant. Of course only processes connected with macroscopically significant energy flows can be described in that way, and even then it is difficult to determine those flows as in the case of metabolic processes such as photo-synthesis. Although photosynthesis is the most vital process, it consumes usually less than five percent of the net radiation and is therefore often ignored when looking at the energy-balance of a plant. Neglecting the fact that a plant consists of many compartments with different processes and therefore functions, that are spatially distributed, the overall energy-balance is:

$$\frac{dU_{pl}}{dT_{pl}} = \Phi_n + G + H + \lambda E + M \quad (7.1)$$

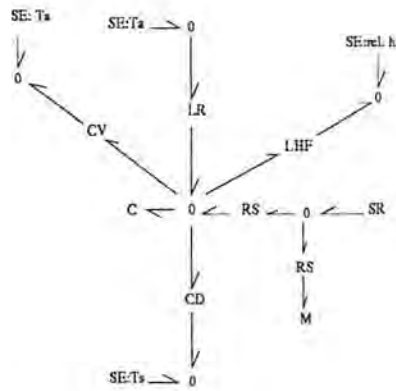


Figure 7.1: bond graph for the energy balance of a plant

It is more accurately the energy balance for a canopy. The approach is often referred to as a big leaf model, since it doesn't take spatial variations of the canopy into account. Φ_n is the net radiation and energy input into the system. G is the heat flux to the ground, M is the energy flux into metabolic storage, H the sensible and λE the latent heat flux. This can be easily reformulated into an entropy balance and put into bond graph notation. The entropy flux connected to a process, that causes either energy to flow into or out of a system equals the energy flux connected to the system divided by the systems absolute temperature. Figure 7.1 show the entropy balance of a plant in bond graph notation. The element CD contains the equations characterizing the heat flux from soil to plant. The element CV describes the convective and conductive heat exchange between atmosphere and plant, while LHF describes the latent heat lost via transpiration. The element LR stands for the energy fluxes connected to long-wave radiation transmitted to and absorbed from a plant's environment. The element SR describes the solar input. Usually the energy balance is used to determine sensible and latent heat fluxes. In this case several simplifying assumptions are made. The energy flux into metabolic storage is neglected. The sensible heat flux between plant and soil is set to be a constant fraction of the net radiation or neglected. This is reasonable, since latent heat flux occurs mainly from the canopy and the energy lost via the pathway leaf-shoot-soil is very small. The remaining terms describe a relation between net radiation, sensible and latent heat fluxes between the plant and the atmosphere. This simplified

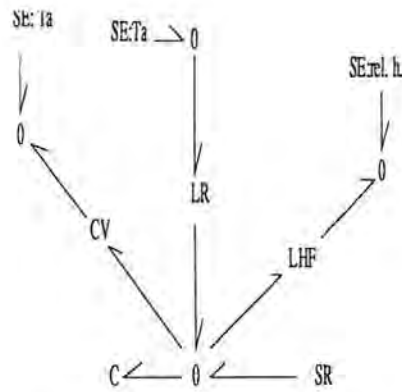


Figure 7.2: bond graph for the energy balance of a plant under steady state conditions

balance is displayed in Figure 7.2. The following sections review models and physical laws commonly used to describe net radiation, sensible heat flux and latent heat flux.

7.1 net radiation

Net radiation is the sum of all long and short-wave radiation, diffuse or beam, that is absorbed by the vegetation cover. The parameters determining net radiation are highly variable. The effects of atmosphere in scattering, absorbing and emitting radiation are variable with time as atmospheric conditions and air mass change. The direction from which diffuse radiation is received is a function of conditions such as cloudiness and atmospheric clarity, which vary greatly. Therefore the energy input into the vegetation is subjected to big fluctuations. Net radiation depends on the leaf angle distribution and the absorption, reflection and transmittance characteristics of the plant canopy, which are dependent on wavelength, incoming radiation angle and physiological characteristics such as leaf age, moisture content. Further the area available for absorption of radiation changes as the sun moves across the sky, since the canopy exists of multi-layered and -directional leaves. Radiation data are the best source of information for estimating average solar radiation. Lacking these data from nearby locations of similar climate, it is possible to use empirical relationships to

approximate incoming flux. The next section reviews two different models of incident solar radiation.

7.1.1 Estimation of average solar radiation

the Angstroem model

The Angstroem model relates average monthly daily data to extraterrestrial radiation on a horizontal surface and to average fraction of possible sunshine hours. It is a good approximation for average incident radiation for a period of several weeks or longer. Data on average hours of sunshine n or average percentage of possible sunshine hours are widely available from many hundreds of stations in many countries [22].

$$R_0 = G_0(c + d\frac{n}{N}) \quad (7.2)$$

The extraterrestrial radiation on a horizontal surface can be calculated from the following equation, using the day of the year I and the latitude ϕ as input:

$$G_0 = \frac{86,400}{\pi} G_{sc} [1 + 0.33 \cos(\frac{360I}{365})] [\cos\phi \cos\delta \sin\omega_s + \frac{2\pi\omega_s}{360} \sin\phi \sin\delta] \quad (7.3)$$

The average day-length N can be calculated as a function of latitude ϕ and sunset hour angle ω_s

$$N = \frac{2}{15} \arccos(\tan\phi \tan\delta) \quad (7.4)$$

$$\delta = 23.45 \sin(360 \frac{284 + I}{365}) \quad (7.5)$$

$$\omega_s = -\tan\phi \tan\delta \quad (7.6)$$

model of Penning de Vries

When modeling transpiration of a plant community it is of interest to have a model for radiation that allows approximations for shorter time frames. The model of Penning de Vries models total clear sky radiation as a function of solar height ($\sin\beta$) and light absorption by the atmospheres, which is a function of solar height and atmospheric absorption κ_{atm} . Cloudy sky radiation is assumed on fifth of clear sky radiation. Solar height can be computed as a function of latitude λ , declination δ_s and daytime t_h . Solar declination δ_s is given as a function of the day of the year:

$$R_0 = 1360 \sin\beta e^{-\frac{\kappa_{atm}}{\sin\beta}} \quad (7.7)$$

$$\sin\beta = \sin\lambda \sin\delta_s + \cos\lambda \cos\delta_s \cos\left[\frac{2\pi}{24}(t_h + 12)\right] \quad (7.8)$$

$$\delta_s = -23.4 \frac{2\pi}{180} \cos\left[\frac{2\pi}{365}(t_d + 10)\right] \quad (7.9)$$

7.1.2 long-wave radiation

Long-wave radiation is emitted by surrounding objects. The radiation they transmit is, if they are black bodies:

$$L = \sigma T_{blackbody}^4 \quad (7.10)$$

Real objects behave more like gray bodies, whose radiation can be described as a fraction ϵ of black body radiation. The main source of long-wave radiation for plants is the sky. Since it does not behave as an ideal black body its long-wave radiation is modeled as:

$$L = \sigma [T_{blackbody} - 20]^4 \quad (7.11)$$

It should be noted that long-wave radiation just as solar is subject to frequent fluctuations and therefore real radiation data is preferable, especially when modeling short time interval's.

considering canopy architecture

Energy input into vegetation cover is dependent on the area available for absorption. Canopies are multi-directional and -layered structures and therefore the area absorbing sunlight changes overtime making the determination of the absorbing area difficult. The simplest model uses horizontal leaves with no overlap. Their area is described by the ratio of leaf to ground area, which is the leaf area index (LAI). A more advanced model is one considering an infinitesimal overlap dL in horizontally distributed leaves. The light intercepted by the canopy then is proportional to the sunlit area $L = 1 - e^{-LAI}$. Models considering overlap and leaf angle distributions other than horizontal project the shadow of the leaves onto a horizontal plane and use this to describe sunlit area as: $L = (1 - e^{-\kappa LAI})/\kappa$. κ is the extinction coefficient. It is dependent on solar elevation and average leaf angle. In practice the geometrically derived extinction coefficient is replaced by an empirically determined constant, with which the effective surface for calculation of radiative energy flux is determined.

considering the spectral properties of leaves

The reflectance, absorptance and transmittance of plants varies over wavelength. Green plants have a very low albedo for photosynthetically active radiation, where chlorophyll absorbs radiation efficiently. Radiation in the wavelength band from 0.4-0.7 μm is effective for photosynthesis. Growing plants absorb more than 90 % of it. At about 0.7 the albedo increases dramatically. Since nearly half of the solar energy that reaches the surface is at wavelengths longer than 0.7 μm this increase in albedo is significant for the energy budget of the surface. Since this is no longer photo-active, the high reflectance helps plants to stay cool. The albedo of vegetated surfaces depends on the texture and physiological conditions of the plant canopy. Leaf canopies with complex geometries and cavities have lower albedos than the individual leaf. The ratio of near infrared to visible radiation decreases with depth below the top of the canopy, because the visible wavelengths are absorbed more efficiently.

Thus the higher albedos of leaves for near infra-red radiation allows it to transcend to the surface. In the study [12] therefore reflectance and transmittance for near-infra-red and visible were determined separately for dead and living vegetation cover respectively, since the albedo for near-infra-red decreases in dead material.

7.2 sensible and latent heat flow between atmosphere-plant

sensible heat flux

The sensible heat flow from a plant or vegetation cover can be described by equation 7.12 assuming that there is no temperature gradient within the plant:

$$H = 2\alpha A_{ground} LAI (T_{veg} - T_a) \quad (7.12)$$

It is proportional to the ground area (A_{ground}), the leaf area index (LAI), the conductance to heat transfer (α) and the temperature difference ($T_{veg} - T_a$) between atmosphere and canopy.

latent heat flux

Using fick's law for one dimensional diffusion the energy flux connected to evaporation is :

$$\lambda E = \lambda g_{diffusion} (c_i - c_a) \quad (7.13)$$

The mass transfer is proportional to the diffusion conductance $g_{diffusion}$ and the concentration difference ($c_i - c_a$) of water vapor between inside the stomata and the atmosphere. The latent heat flux is the mass flow times the specific heat for evaporation of water. A more useful formulation is one using the difference in water-vapor-pressures.

$$\lambda E = \lambda g_{diffusion} 0.622 \rho_a [p_w(T_{veg}) - p_w(T_a)] / P \quad (7.14)$$

It is further assumed that the air inside the pore is saturated .

$$\lambda E = \lambda g_{diffusion} 0.622 \rho_a [p_{ws}(T_{veg}) - p_w(T_a)] / P \quad (7.15)$$

The diffusion coefficient consist of a resistance to diffusion of the stomata and a resistance to diffusion in the atmosphere. Stomatal resistance to mass transfer is briefly reviewed in Chapter 5.

aerodynamic resistances resistance

In nature most of the time heat and mass transfer is turbulent, in contrast to greenhouses were the movement of air is greatly reduced. Therefore laminar flow can be assumed in greenhouses.

In GCMs generally three resistances under turbulent conditions are considered: a resistance toward the boundary layer, a resistance within the turbulent transition layer above the canopy and a resistance within the canopy air spaces (see [13], p. 684). GCMs devide the atmosphere into the conventional constant-stress layer, a turbulent transition layer, a boundary layer and canopy air spaces. The resistance of the boundary layer can be modeled as:

$$r_{bl} = C_1 / \sqrt{u_t} \quad (7.16)$$

It is proportional to a bulk boundary resistance coefficient and the the wind speed at the height t, where the turbulent transition layer begins. It is dependent on vegetation type. In turbulent conditions the resistance in the transition layer for heat and mass transfer can be estimated by resistance for momentum. The resistance for momentum is calculated with the wind-speed at height z. The resistance between reference height $z(0) = d + z_0$ and the height z can be calculated as:

$$r_a = \frac{1}{\kappa^2 u_z} \left[\ln \frac{z - d}{z_0} \right]^2 \quad (7.17)$$

The reference height can be seen as the sink for momentum.

7.3 Implementation of the energy balance in Dymola

The energy-balance was implemented in Dymola for the simulations of sensible and latent heat flux between a vegetation cover and the atmosphere and to determine canopy temperature. The program describes the energy balance of a vegetation cover using ambient temperature T_a , humidity hum , solar radiation s and long-wave radiation exchange between sky and cover as inputs. The vegetation cover is modeled as a single absorbing and emitting layer with a leaf area index of two and a light extinction coefficient of $\kappa = 0.6$. The properties of areas of bare soil were not considered, values for the vegetation cover were applied to $2500m^2$ of ground area. Energy exchange between canopy and ground was neglected.

Some of models reviewed earlier were used to describe the different components of the energy balance. Latent heat flux was modeled with Fick's diffusion law. A stomatal conductance found in [4] was implemented and the aerodynamic resistance was modeled in a simplified form of resistances found in [13].

The program consists of a library, containing the different submodels, the main model, which connects the different compartments and defines cuts and inputs, the appendix containing data on radiation and humidity, and a command file that generates ACSL code in Dymola.

the main model

The main model `veg.dym` uses the submodel `SUNv` to describe the solar radiation absorbed by the cover. Incident radiation data is found in the table `RAD` in the `veg.app` file. The long-wave radiation exchange between vegetation and sky is characterized in the submodel `radexchange`. It was taken from the study [24] and modeled as the radiation absorbed and transmitted by two black bodies, one of which has an infinitely large absorption area. The model convection was also taken from [24] using the resistance to momentum in the

atmosphere to determine sensible heat transfer. Submodel latent holds equations for latent heat flux using Fick's law of diffusion to describe heat flux connected to mass transfer of water vapor, using submodel stomres for the stomatal resistance and model blres to model aerodynamic resistance. Submodel c describes the thermal capacity of the vegetation cover.

the library model and parameterizations

The library contains the different submodels used in the main program. Model class parameter contains parameters, that are common to many submodels. Since this model is quite simple it only contains the value of the ground area $ground = 2500m^2$. The model bond describes the structure of bonds. TwoPort is also a structural model, that can be used for any model having two ports.

LW describes blackbody radiation emitted from a body. Skyveg contains the effective emitting area. Radexchange models total long-wave radiation. In the case of the sky having a close to infinite area (compared to the ground area), it is given the effective emitting area of the vegetation cover.

Sensible heat flux is described with the submodel convection, it uses the submodel sensveg1. Sensveg1 is of the class sensible and defines the convection conductance G_o . Sensible is a structural component. The model convection uses the formula for convection between a plane and atmosphere. The submodel SE defines an effort source. Ambient temperature and humidity were modeled as effort sources.

Submodel Sunv describes absorption of solar energy by the vegetation. A reflectance of $\rho_{veg}=0.3$, a leaf area index of LAI and a light extinction coefficient of $\kappa=0.6$ were assumed. Solar incident radiation on a horizontal plane was taken from data provided in the dec-file.

The model capacitor describes the thermal capacity of the vegetation cover. The change

in internal energy equals the change in canopy temperature times its mass and specific heat capacity. The mass of the system was assumed to be 100 tons. The specific heat capacity was set to be that of water. This capacity equals a capacity of a layer of 4 cm of water.

The model stomres describes the stomatal resistance water vapor encounters on its way to bulk air. The model was taken from study [4]. It models stomatal resistance dependent on incoming short-wave s , leaf area index LAI and a factor r_0 , that is dependent on vegetation and climate. Since r_0 was unknown it was set to 1.0.

Resistance encountered in the atmosphere is characterized in submodel bres. It consists of a resistance of the boundary layer and a resistance in the turbulent transition layer. Resistance within the canopy was neglected. Equations for both resistances were taken from [13], page 684. The resistance of the boundary layer is dependent on a vegetation type specific constant c_1 and the wind speed u_t at the height where the turbulent transition layer begins. C_1 was set to one and u_t was set to be the same as the wind speed u at reference height. The resistance in the turbulent transition layer is described with equation 7.17. Reference height was chosen as 0.2m above canopy, as proposed by [9], page 475. Vegetation height h was set to 1.0m. Wind speed was modeled as a sinus function peaking at dawn and dusk.

Model class latent models the latent heat flux between the vegetation and the cover. Latent heat flux equals the evaporation rate time the specific evaporation heat $\lambda = 2500 \text{ kJ/kg}$. evaporation is driven by the water vapor difference between inside the stomata and bulk air. The water vapor inside the stomata p_{sv} is assumed to be saturated. The water vapor outside p_w equals the relative humidity times the saturation water vapor p_{ws} pressure at ambient temperature T_a . The constants a, b, c determine the saturation-water vapor pressure curve in Pa. The density of air ρ_a is set to 1.204 kg/m^3 and the ambient pressure P is assumed constant at 1 bar.

error sources and result evaluations

The parameters c_1 and r_0 , had to be set to dummy number of 1.0 , since their range was unknown. Their values have an effect on values of stomatal and aerodynamic resistance. The wind speed at reference height and at the end of the boundary layer were set to be the same. Wind speed increases logarithmally with height. This too, will effect the values of aerodynamic resistance. Rough estimates were made for the heat capacity of the vegetation layer, the range of wind speed and temperature.

The inputs also are an error source. Radiation data and humidity were taken from one specific site, but temperature and wind speed were modeled as cosine functions. Temperature influences humidity and radiation influences temperature. Therefore, if one uses them as effort sources, the data has to be from one site and day.

Results obtained from these assumptions showed a nearly constant vegetation temperature throughout the day. This is due to the high capacity assumed. If the capacity is set lower the plant temperature will start to change. The bowen ratio was minimal at noon with a value of hundred. The bowen ratio is the ratio of sensible to latent heat flux. It is around 0.1 for tropical rain forest and around 10 for desert. The magnitude of this value indicates, that the resistance for heat transfer is much to low. Latent heat flux is zero during the night, because transpiration ceases during night time. Sensible heat flux from vegetation to the atmosphere is negative during the night and positive during day time.

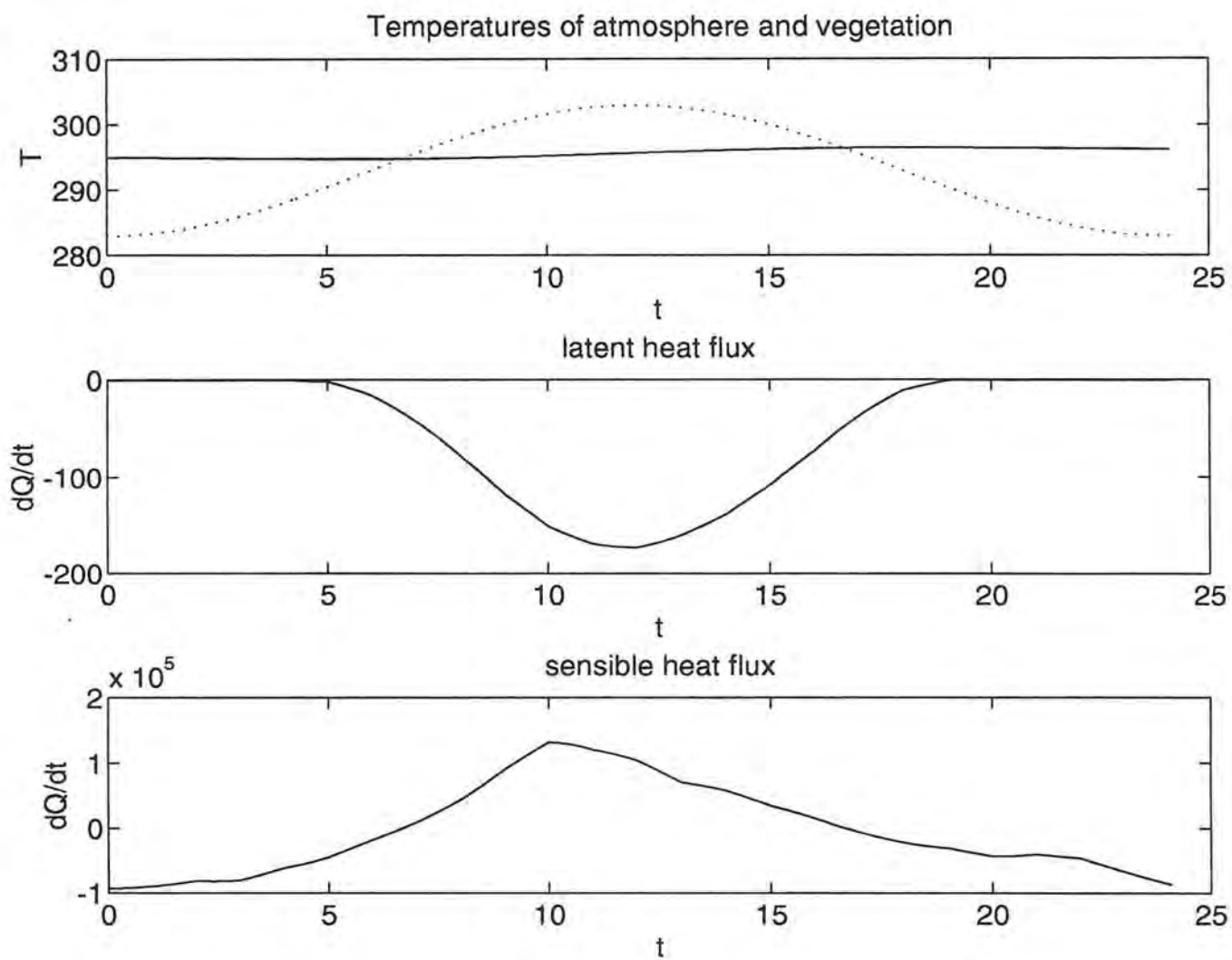


Figure 7.3: simulation run for a capacity of $4.19e5 kJ/K$

7.4 The Penman-Monteith equation

When modeling vegetation the canopy temperature is often unknown. Therefore in plant physiology the Penman-Monteith equation is used. The Penman Moneith equation uses fick's law for one-dimensional diffusion of water-vapor and the energy balance to approximate the evaporation rate from a vegetation cover. By using both equations the knowledge of the vegetation-temperature is not needed.

Derivation

It does that by approximating the term of $[p_{ws}(T_{veg}) - p_w(T_a)]$ as $[p_{ws}(T_a) - p_w(T_a)] - s(T_{veg} - T_a)$. S is the slope of the saturation water-vapor pressure curve. The the energy balance is solved for the temperature difference $(T_{veg} - T_a)$ and substituted for the same term in the diffusion equation. For the energy balance the following assumptions are made. The plant is in steady state. The fluxes into metabolic storage and ground are negible. Therefore the fluxes considered are net radiation, the latent and sensible heat flux. The transpiration rate is derived by the Penman-Monteith as:

$$E = \frac{s\Phi_n + \rho_a c_p \alpha (p_{ws}(T_a) - p_w(T_a))}{\lambda [s + (\gamma \alpha / g_{diffusion})]} \quad (7.18)$$

imposed evaporation

Under turbulent conditions the conductance of heat and mass is very good and the vegetation is said to be well coupled to the environment. In this case the leaf temperature will approach the temperature of its environment. It is well coupled to its environment. The above equation is reduced to :

$$E = \frac{\rho_a c_p}{\lambda \gamma} g_s (p_{ws}(T_a) - p_w(T_a)). \quad (7.19)$$

In this case evaporation is determined by the stomatal conductance g_s and the water vapor deficit in the atmosphere.

equilibrium evaporation

On the other hand, if wind speed is very small, boundary layer resistance is very big and the transfer of heat and mass to the atmosphere is poor, as e.g. in a greenhouse. Then the vegetation is poorly coupled to its environment. Here the Penman-Monteith reduces to :

$$E = s\Phi_n/\lambda(s + \gamma) \quad (7.20)$$

This means that the influence of stomata or atmospheric water vapor pressure is insignificant. This can be explained as follows. Picture a green house with little or no air movement. When there is radiation input into the glass-house, temperature increases, the water vapor holding capacity increases, so that it is possible to maintain a constant leaf to air pressure difference, even though the vapor pressure of the air in the glass-house may be continually increasing. This steady-state evaporation depends on the rate of energy input into the system.

These two cases are extrema rarely reached. In vegetation modeling therefore a fraction coefficient ω is used to characterize evaporation, with $\omega = 1$ indicating pure equilibrium transpiration.

Conclusions

This research is a first step in using bond graphs for modeling and simulating plant biosystems. Bond graphs can be used for the description of micro mechanisms that determine system behavior in vegetation, or they can be used to describe overall system behavior. For both models analyzed in this report the overall system response was of interest. The system boundary was drawn around a single plant in the hydraulic flow model and around a plant community in the big leaf model.

Biological models use physical laws to describe interactions between the plant and its environment or to describe mechanisms on cellular level. Overall plant behavior often is captured with empirical relations. In many cases, as for example in agriculture or forestry the translocation of organic matter is of importance. It is described with help of mass balances. The specific energy for translocation to the different compartments and for the transformation reactions from one organic compound to another are of less importance. These models cannot be put into bond graph notation. In the last decade a lot of effort has been made to take thermodynamics into account when modeling biological processes. This approach can make use of bond graph modeling.

When bond graphs represent mechanisms on cellular level, the use is mainly conceptual. Upscaling from cellular to overall plant responses - given quantitative results are found - is extremely difficult. Therefore mechanistic models are the more efficient way in modeling overall plant responses. Mechanistic models attempt to describe the processes, that determine dynamic development of a system physically correct. They formulate rate of changes of the state variables in terms of differential equations. The mathematical relationship is dictated by the elements and the structure of the system, which are highly nonlinear in many cases. [25].

One of the major problems, that has to be faced in plant modeling is the correct parameterization describing biological behavior. The behavior is influenced by environmental and

physiological conditions. These conditions are subjected to diurnal and seasonal changes. Daily changes are mainly in environmental conditions, while seasonal are in both. For example the flow in a root is dependent on temperature, precipitation, soil moisture, and nutrient supply, which are environmental conditions. It is also dependent on plant species, health and age. Parameter ranges that describe the different conditions are probably very hard to determine and do not exist. Therefore studies modeling and simulating plant behavior are limited to very narrow sets of conditions. Calculations are mostly done for one specific plant and day.

The hydraulic flow model is a mechanistic model. Water flow through a plant is analyzed by introducing resistances and storages for the different plant parts. With help of this model the functionality of different plant parts in handling water supplies becomes evident and the daily water cycle in a plant is determined. As mentioned earlier many studies only consider a time-frame of a few days. Models running for a longer time would have to account for tissue growth, changing functionality, e.g. as sap wood turns to core wood, health, events, e.g. leaf loss due to temperature dropping below 10 degrees Celsius and others. These processes have a effect on the parameters for the different resistances and capacitances. Describing their changes over time requires a tremendous set of data and it is dubious, if conclusions drawn from such an experiment are worth the effort.

The energy balance for a plant or plant community is used in ecology for modeling the interactions between atmosphere and vegetation. The environment is commonly split into atmosphere, one or two layers of vegetation and several layers of soil. The modeling effort lies not so much in the description of the energy fluxes between compartments, but in determining the influencing factors, as for example the stomatal resistance. Sets of parameters accounting for vegetation type and different climates exist. Nevertheless, accurate models require site specific factors, causing a considerable amount of effort for measurements and model calibration. The approach in this study was to take models of energy transfer mechanisms found in ecological modeling literature and reformulate them into bond graph notation.

This information then can be used in projects like [24], which models the energy fluxes between different subsystems of Biosphere 2, as for example vegetation and atmosphere, or atmosphere and air handlers.

The next step in modeling the thermal behavior of the vegetation layer would be introducing more sophisticated models for conductance of the stomata and boundary layer to use it with a set of temperature, humidity and radiation from one specific sight. Further the introduction of nodes modeling the energy balances of atmosphere and soil layers could replace the effort sources now dictating the behavior of the plant cover.

Bibliography

- [1] R.R. Allen, *bond graphs in biosystems*, computer programs in biomedicine, vol. 318 no.2, pp148-216, 1978.
- [2] F.E. Cellier, *continuous system modeling*, Springer-Verlag, 1991.
- [3] C.Edwards, D.A. Rose, *mathematics and plant physiology*, Academic Press, 1995.
- [4] M.G. Incan, R. Forkel, *comparison of energy fluxes calculated with the penmanmonteith equation and the vegetation models of SiB and Cupid*, Journal of Hydrology 166, pp 193-211, 1995.
- [5] I.R. Johnson, J.J. Melkonian, J. H. Melkonian, J.M. Thornley & S.J. Riha, *a model of water flow through plants incorporation shoot & root 'message control of stomatal conductance*, Plant, Cell and Environment, Vol. 14, pp531-544, 1991.
- [6] H.G. Jones, *plants and micro climate*, Cambrigde University Press, 1992.
- [7] P.J. Kramer,S. Boyer, *Water relations of plants and soils*, Academic Press 1995.
- [8] P.S. Nobel, *transpiration stream of desert species: resistances and capacitances for a C₃ a C₄ and a CAM plant*, Journal of experimental botany, Vol. 34, No.147, pp 1379-1391, 1983.
- [9] P.S. Nobel, *physiochemical and environmental physiology*, Academic Press 1991

- [10] G.F. Oster, A.S. Perelson, A. Katchalsky, *network thermodynamics: dynamic modeling of biophysical systems*, Q. Rev. Biophysics, Vol.6, pp. 1-134, 1973.
- [11] F.W.T. Penning de Vries, H.H. Van Laar, *simulation of plant growth and crop production*, Pudoc Centre for Agricultural Publishing and Documentation, Wageningen, 308pp, 1982.
- [12] P.J. Sellers et al. *a revised land surface parameterization (SiB2) for atmospheric GCMs. Part 2: the generation of global fields of terrestrial biophysical parameters from satellite data*, Journal of Climate, Vol. 9, No.4, 1996.
- [13] P. J. Sellers et al., *a revised land surface parameterization (SiB2) for atmospheric GCMs. Part1: Model Formulation*, Journal of Climate, Vol, No.4, April 1996.
- [14] J.A.C. Smith, *water deficits*, environmental plant biology 1993.
- [15] J.A.C. Smith, P.J. Schulte, P.S. Nobel, *water flow and water storage in agave deserti: osmotic implications of crassulean acid metabolism*, Plant, Cell and Environment, Vol 10, pp. 639-648, 1987.
- [16] O.Taconet, R.Bernhard, D. Vidal-Meltjar, *evaporation of an agricultural region using a surface flux/temperature model based on NOAA-AVHRR data*, J.Clim.Appl. Meteorol., 25: 284-307, 1986.
- [17] M. T. Tyree, *a dynamic model for water flow in a single tree: evidence that models must account for hydraulic architecture*, Tree Physiology 4, 195-217, 1988.
- [18] M.H. Zimmermann, *xylem structure and the ascent of sap*, Springer-Verlag 1981.
- [19] J.L. Monteith & M. H. Unsworth *principles of environmental physics*, 2nd edition, London: Edward Arnold, 1990.
- [20] H. Mohr, P. Schopfer, *plant physiology*, Springer-Verlag, 1995.

- [21] L. R. Ahuja, R. D. Williams, *scaling water characteristic and hydraulic conductivity based on Gregson-Hector-McGowan approach*, soil sci. soc. Am. J., 55:308-319, 1991.
- [22] J.A. Duffie, W.A. Beckmann, *solar engineering of thermal processes*, Wiley Interscience, 1991.
- [23] G.H. Smerage, *matter and energy flow in biology and ecological systems*, Journal of theor. Biology, 57, 203-223, 1976.
- [24] F.E. Cellier, F. Mugica, A. Nebot, *modeing the thermal behavior of Biospher2 in a non-controlled environment using bond graphs*
- [25] H.Bossel, *mathematical model, program documentation and simulation results*, Treedym 3, Bericht des Forschungszentrums Waldoekosysteme, Reihe B, Bd.35, 1994.

Table 7.1: Table of abbreviations

A_{ground}	m^2	Ground area
a_j		activity of species j
a,b	-	statistical coefficients dependent on climate
c_i	-	concentration of water vapor inside the stomatal pores
c_a	-	concentration of water vapor atmosphere
c_p	kJ/kgK	specific heat capacity of water
$d = 0.64h$	m	zero-plane displacement
e	V	electrical potential
E	m^3/s	evaporation rate
F		Faraday's constant
g	m/s^2	gravitational constant
$g_{diffusion}$	Pas/m^3	the conductance to water-vapor along the path:leaf pore-stomata-boundary layer-bulk air
g_s	Pas/m^3	stomatal conductance
G	W/m^2	sensible heat flow plant-soil
G_0	W/m^2	extraterrestrial solar radiation on a horizontal plane
G_{sc}	W/m^2	solar constant
H	W/m^2	sensible heat flow plant-atmosphere
h	m	height
h_v	m	average vegetation height
I	-	day of the year
$k = 0.41$		von Karman constant
LAI	-	Leaf area index
m	kg	mass
M	W/m^2	net energy flow into metabolic storage
P	Pa	atmospheric pressure

$p_w(T_a)$	Pa	water vapor pressure atmosphere
$p_w(T_{veg})$	Pa	water vapor pressure inside stomata
$p_{ws}(T_{veg})$	Pa	saturated water vapor pressure at T_{veg}
$p_{ws}(T_a)$	Pa	saturated water vapor pressure at T_a
R	kJ/kmolK	ideal gas constant
R_0	W/m^2	global radiation incident to a plane
r_0	-	upper limit for resistance, depending on season and vegetation type
r_{bl}	-	boundary layer resistance
s	W/m^2	incoming short wave radiation
t	m	height at which turbulent transition layer begins
T	K	absolute temperature
T_{pl}	K	Temperature of the plant
T_{veg}	K	Temperature vegetation
T_a	K	Temperature bulk air
U_{pl}	kJ	internal energy plant
u_*	m/s	friction velocity
u_t	m/s	speed at height t
u_z	m/s	speed at height z
V_w	$m^3/kmol$	molar volume of water
z_j	-	is an integer representing the charge number
$z_0 = 0.13h$	m	roughness length
α	W/m^2K	heat conductance plant-surface-atmosphere
γ	Pa/K	psychrometric constant
λ	kJ/kgK	specific heat for evaporation of water
Φ_n	W	net radiation absorbed by the Plant
ϕ	-	latitude of site
Ψ	Pa	water potential
θ	%	relative water content

Appendix A

plots

-	root
:	stem
-	water storage parenchyma
-.	inner chlorenchyma
-	outer chlorenchyma

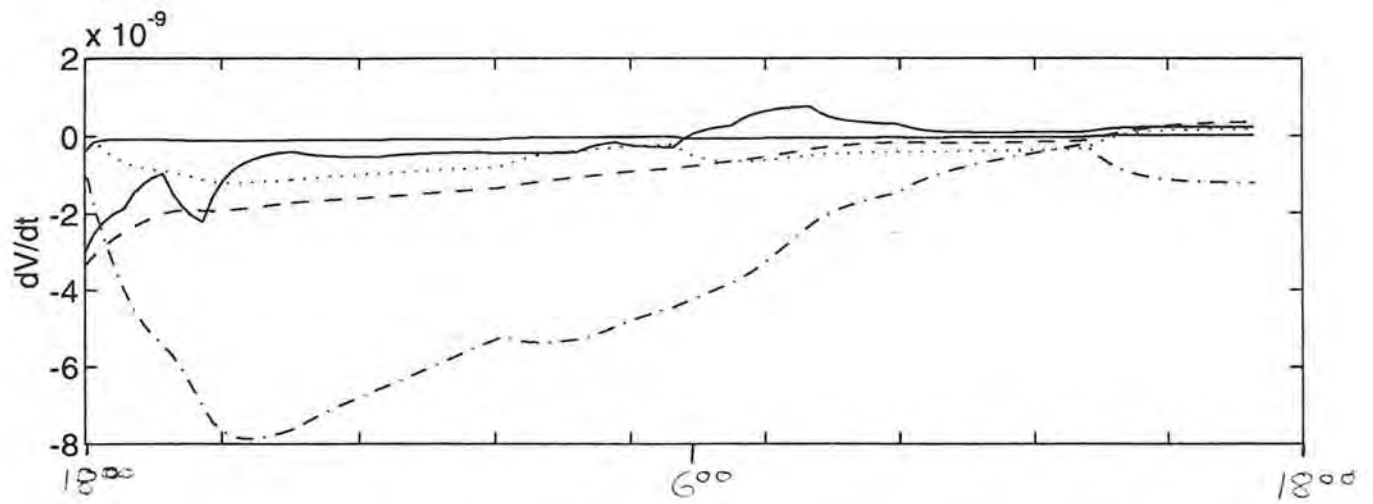


Figure A.1: waterflow into and out of storage

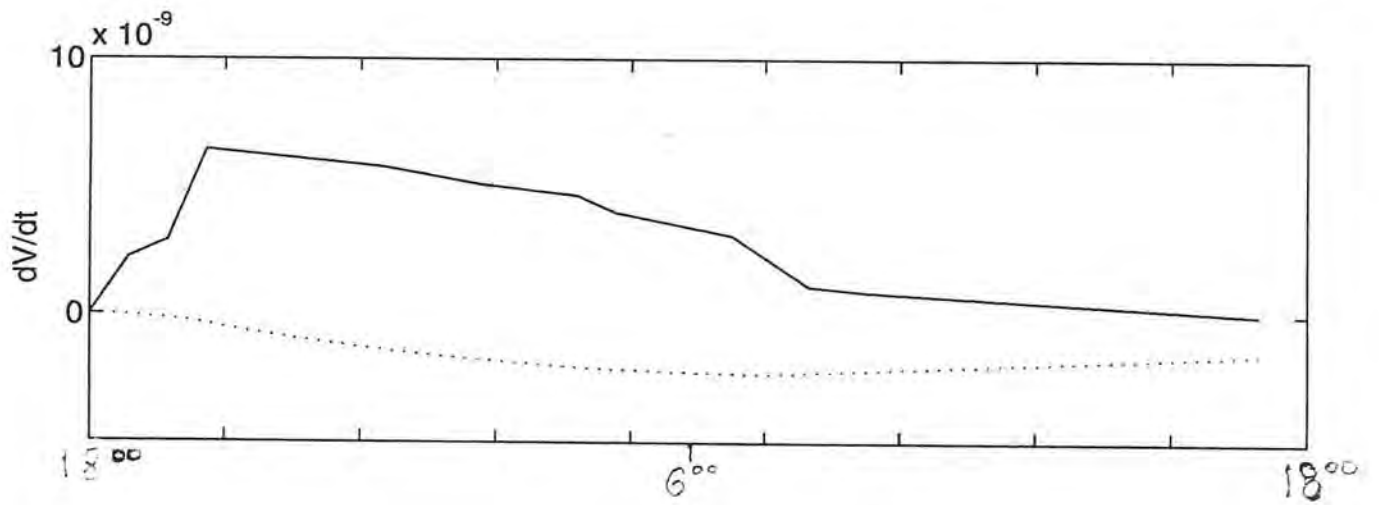


Figure A.2: transpiration and uptake by the root

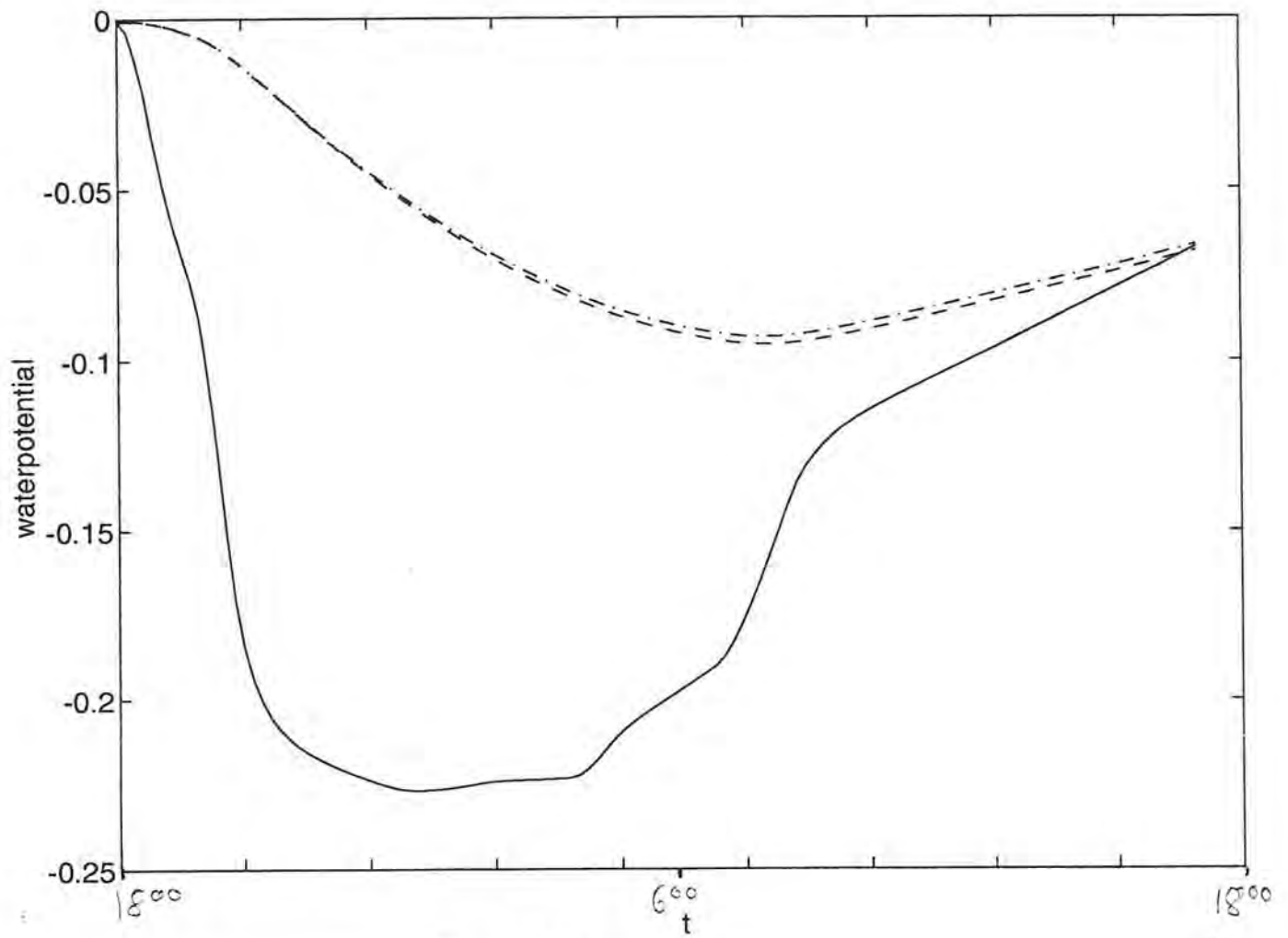


Figure A.3: water potential

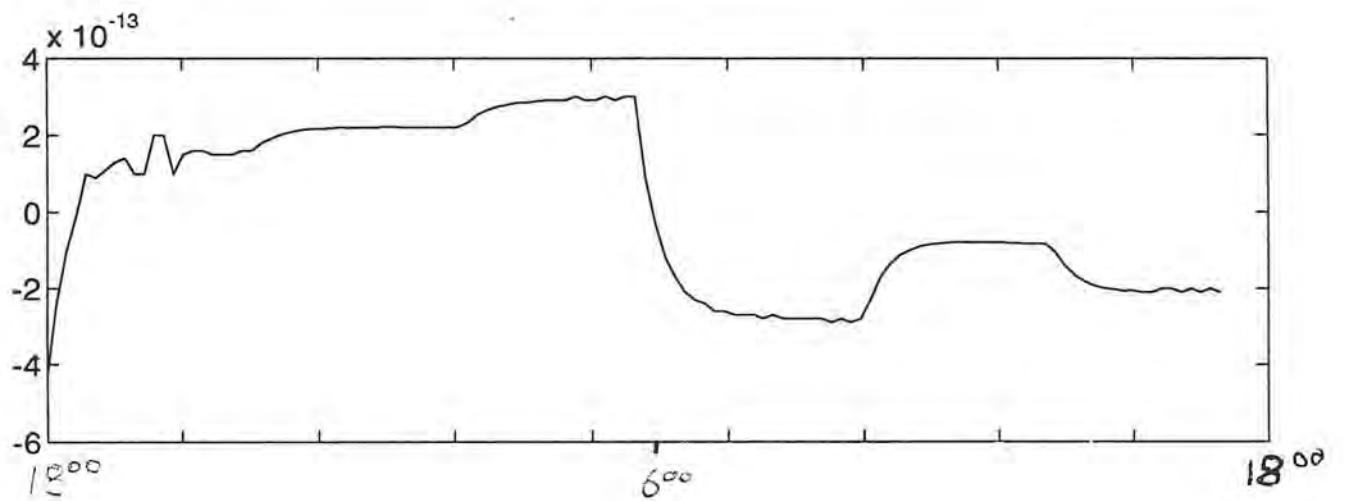


Figure A.4: difference in wateruptake for the outer chlorenchyma between simulations run with constant and variable osmotic pressure

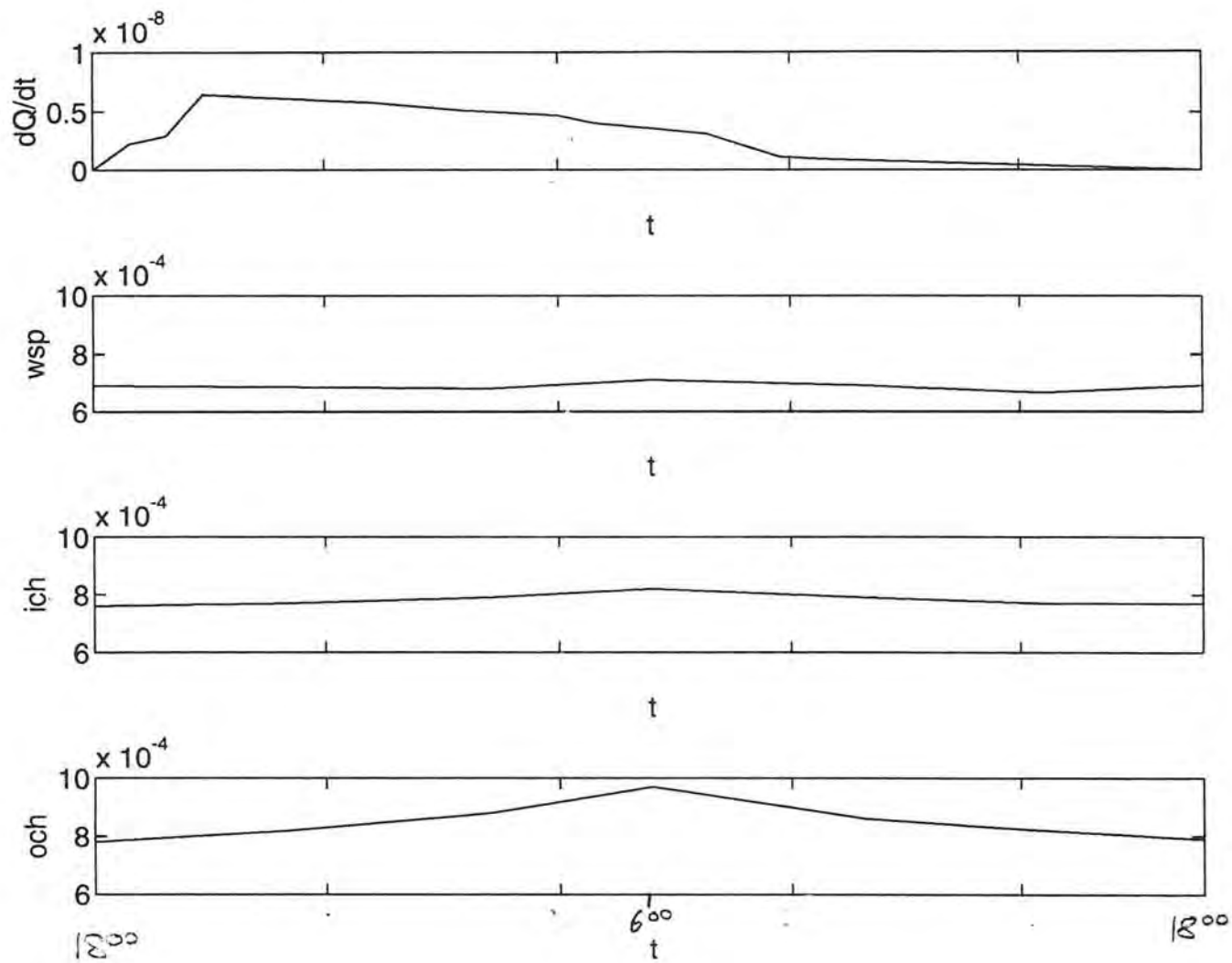


Figure A.5: transpiration rate and osmotic potential

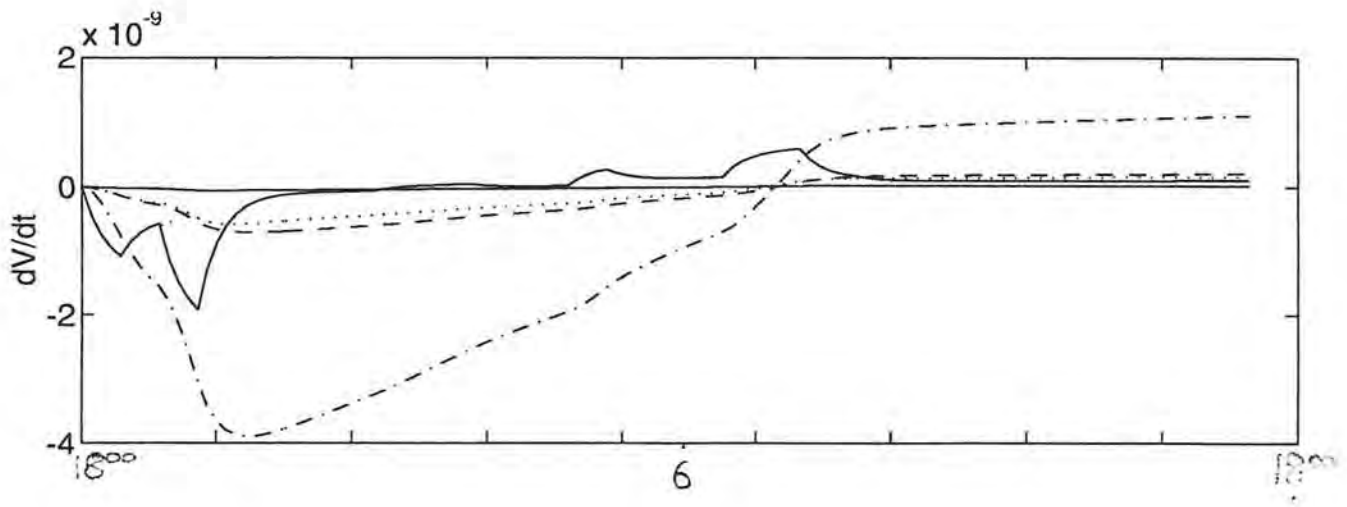


Figure A.6: water flow out of storage

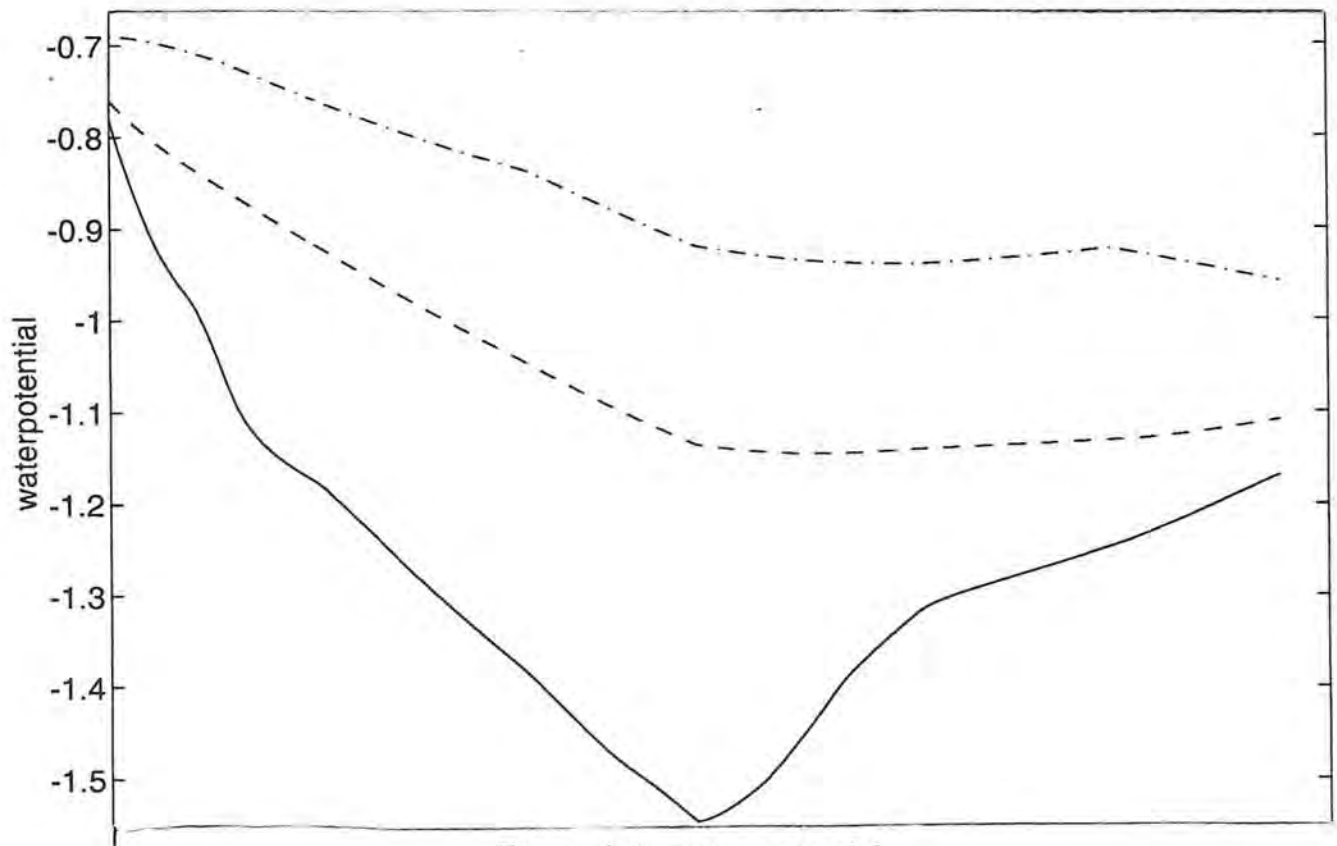


Figure A.7: water potential

Appendix B

programs

B.1 program:agave.dym

```
model agave9
submodel (G) sr (G=3.601e7), xylem1 (G=1.75e6), xylem2 (G=2.22e6),
xylem3 (G=8.78e5), xylem4 (G=2.8698e7), ochr (G=2.86e7), roots (G=2.6e7),
stems (G=8.9e6), wsps (G=2.48e6), ichs (G=1.98e7)
submodel (SF) soil, root, stem, wsp, ich, och
submodel (SE) transpir
submodel (I) croot (I=1.8e-5), cstem (I=1.8e-4), cwsp (I=1.2e-3),
cich (I=2.19e-4), coch (I=5.54e-5)
submodel (bond) b1, b2, b3, b4, b5, b6, b7, b8, b9, b10, b11, b12, b13, b14, b15
node n1, n2, n3, n4, n5, n6, n7, n8, n9, n10, n11, e1, e2, e3, e4, e5
output x1, x2, x3, x4, x5, x6, x7, x8, x9, x10, x11, x12, x13, x14
output x15, x16, x17, x18
```

{connecting elements}

connect sr at n1

connect soil at n1

connect roots at n2

connect root at n2

connect croot at n2

connect stems at n4

connect stem at n4

connect cstem at n4

connect wsps at n6

connect wsp at n6

connect cwsp at n6

connect ichs at n8

connect ich at n8

connect cich at n8

connect och at n10

connect coch at n10

connect xylem1 at n3

connect xylem2 at n5

connect xylem3 at n7

connect xylem4 at n9

```
connect ochr at n11
```

```
connect transpir at n11
```

```
{connecting the bonds}
```

```
connect b1 from n1 to e1
```

```
connect b2 from n2 to e1
```

```
connect b3 from e1 to n3
```

```
connect b4 from n3 to e2
```

```
connect b5 from n4 to e2
```

```
connect b6 from e2 to n5
```

```
connect b7 from n5 to e3
```

```
connect b8 from n6 to e3
```

```
connect b9 from e3 to n7
```

```
connect b10 from n7 to e4
```

```
connect b11 from n8 to e4
```

```
connect b12 from e4 to n9
```

```
connect b13 from n9 to e5
```

```
connect b14 from n10 to e5
```

```
connect b15 from e5 to n11
```

```
{inputs}
```

```
transpir.E0=-tra(Time)
```

```
soil.F0= -0.4
```

```
root.F0= -0.67
```

```
stem.F0= -0.67
```

```
{wsp.F0= -0.67}
```

wsp.F0=- w(Time)

{ich.F0= -0.76}

ich.F0=- i(Time)

{och.F0= -0.78}

och.F0= - o(Time)

{outputs:}

{turgor pressure}

x1=croot.f

x2=cstem.f

x3=cwsp.f

x4=cich.f

x5=coch.f

{inputs}

x6=transpir.E0

x7=wsp.F0

x8=ich.F0

x9=och.F0

{waterflow tissue layers}

x10=croot.e

x11=cstem.e

x12=cwsp.e

x13=cich.e

x14=coch.e

```
{waterpotential leaves}
```

```
x15=cwsp.f+wsp.F0
```

```
x16=cich.f+ich.F0
```

```
x17=coch.f+och.F0
```

```
{wateruptake root}
```

```
x18=sr.e
```

```
end
```

B.2 program bond.lib

```
{library for elements}
```

```
{ Bond Graph resistor }
```

```
model type R  
  main cut A(e/f)  
  parameter R=1.0  
  R*f = e  
end
```

```
{ Bond Graph conductance }
```

```
model type G  
  main cut A(e/f)  
  parameter G=1.0  
  G*e = f  
end
```

```
{ Bond Graph capacitor/compliance }
```

```
model type C  
  main cut A(e/f)  
  parameter C=1.0  
  C*der(e) = f
```

end

{ Bond Graph inductor/inertia }

model type I

main cut A(e/f)

parameter I=1.0

$I \cdot \text{der}(f) = e$

end

{ Bond Graph effort source }

model type SE

main cut A(e/.)

terminal E0

$E0 = e$

end

{ Bond Graph flow source }

model type SF

main cut A(./-f)

terminal F0

$F0 = f$

end

```
{ Bond Graph of a transformer }
```

```
model type TF
```

```
cut A(e1/f1), B(e2/-f2)
```

```
main cut C[A,B]
```

```
main path P<A-B>
```

```
parameter m=1.0
```

```
e1 = m*e2
```

```
f2 = m*f1
```

```
end
```

```
{ Bond Graph of a gyrator }
```

```
model type GY
```

```
cut A(e1/f1), B(e2/-f2)
```

```
main cut C[A,B]
```

```
main path P<A-B>
```

```
parameter r=1.0
```

```
e1 = r*f2
```

```
e2 = r*f1
```

```
end
```

```
{ Bond Graph bond }
```

```
model type bond
  cut A (x/y), B(y/-x)
  main cut C[A,B]
  main path P<A-B>
end
```

B.3 agave.dec

```
nsteps nstep=5000
```

```
table tra, 1, 13/ 0.0, 2880, 5760.0, 8640.0, 21600.0, &  
                28800.0, 36000.0, 38880.0, 43200.0, &  
                47520.0, 53280.0, 57600.0, 86400.0, &  
                0.0, 2.22e-9, 2.89e-9, 6.44e-9, 5.78e-9, &  
                5.11e-9, 4.67e-9, 4.0e-9, 3.56e-9, 3.11e-9,&  
                1.11e-9, 0.89e-9, 0.0 /
```

```
table o, 1, 7/ 0.0, 15330.0, 30660.0, 43200.0, 59920.0, &  
              73860.0, 86400.0, 0.78,0.8,0.88,0.97, &  
              0.86, 0.82, 0.79/
```

```
table i, 1, 7/ 0.0, 15330.0, 30660.0, 43200.0, 59920.0, &  
              73860.0, 86400.0, 0.76, 0.77,0.79, 0.82, &  
              0.79, 0.77, 0.76/
```

```
table w, 1, 7/ 0.0, 15330.0, 30660.0, 43200.0, 59920.0, &  
              73860.0, 86400.0, 0.69, 0.685, 0.68, 0.71 &  
              0.69, 0.665, 0.69/
```

B.4 program:agave.dyc

```
set Eliminate on
set AutoFileName off
set ShowFullName on
set Events on
{set CommonOn}

enter model
@bond.lib
@agave9.dym

variable value croot.f=0.17, cstem=0.17, cwsp.f=0.19, cich.f=0.26 ,
coch.f=0.28

output equations
outfile agave9.eq
partition

outfile agave9.seq
    output sorted equations
outfile agave9.sleq
    output solved equations

simulation StopTime=86400, algorithm=4, Interval=720
language ACSL
```

```
outfile agave9.csl
```

```
output model
```

```
outfile agave9.cmd
```

```
output experiment
```

```
quit
```

B.5 program:veg.dym

```
model veg
submodel (SE) Ta1, Ta2, hum
submodel SUNv
submodel radexchange
submodel convection
submodel latent
submodel c
submodel blres
submodel stomres
node n1, n2, n3, n4
output x1, x2, x3, x4
connect Ta1 at n1
connect convection from n1 to n2
connect c at n2
connect SUNv at n2
connect Ta2 at n3
connect radexchange from n3 to n2
connect latent from n2 to n4
connect hum at n4

-

{cuts}
convection::sensveg1.rb= blres.rb
latent.rb = blres.rb
latent.rs = stomres.rs
latent.Ta = Ta1.E0
```

```

stomres.I0= SUNv.I0

{inputs}
SUNv.I0= RAD(Time)
{Ta1.E0= Ta(Time)}
Ta1.E0= 293 - 10* cos (Time /24 *2*3.141)
{Ta2.E0= Ta(Time)}
Ta2.E0= Ta1.E0
hum.E0= humidity(Time)
{hum.E0=0.73}
{atmospheric pressure}
latent.P=10e5
{vegetation height}
blres.h=1.0
{windspeed}
blres.u= 5+5*sin(2*3.141/24*Time)
{reference height above canopy}
blres.b=0.2
{c1:bulk canopy boundary-layer coefficient}
blres.c1=1.0

{outputs}
x1=latent.E
x2=convection.e1
x3= convection.f1
x4=c.e
end

```


B.6 program:veg.lib

```
{Physical parameters}
```

```
model class PAR
```

```
parameter ground=2500
```

```
end
```

```
{ Generic Bond Graph TwoPort Model }
```

```
model class bond
```

```
cut A(x/y), B(y/-x)
```

```
main cut C[A,B]
```

```
main path P<A-B>
```

```
end
```

```
model class (PAR) TwoPort
```

```
cut A(e1/f1), B(e2/-f2)
```

```
main cut C[A,B]
```

```
main path P<A - B>
```

```
end
```

```
{ Generic Bond Graph modulated radiation }
```

```
model class (TwoPort) LW
```

```
local G, G0
```

```
parameter sigma=5.67e-8
```

```
G*e1 = f1
```

```
e1*f1 = e2*f2
```

```

    G = G0*sgma*(e1**2)
end

{ Generic Bond Graph modulated convection (Sensible Heat) }

model class (TwoPort) sensible
    local G, G0
    G*e1 = f1
    e1*f1 = e2*f2
    G = G0/(e1 + e2)
end

{Capacitor}
model class c
    main cut A(e/f)
    parameter m=10e5, cp=4.19
    local c, t
    t= m*cp
    c=t/e
    c*der(e)=f
end

{ Bond Graph effort source }

model type SE
    main cut A(e/.)
    terminal E0
    E0 = e

```

end

{ Solar radiation absorbed by VEGETATION }

model class SUNv

main cut A(e/-f)

parameter ground=2500, LAI=2, kappa=0.6, rhoveg=0.3

terminal I0

local s

s= ground*(1. - exp(-kappa*LAI))/kappa*I0*(1-rhoveg)

s=e*f

end

model class blres

terminal u, h, rb, b, c1

local d, z0,z, ra, rbl

parameter k=0.41

{reference height+ vegetation height}

z= b+h

{Typical values of z0 and d see Jones page.67}

z0= 0.13*h

d= 0.64*h

{aeroresistance for monentum in turbulent transition layer}

ra=1/k**2/u*(ln((z-d)/z0))**2

{boundary layer resistance}

rbl=c1*u**(-0.5)

```
rb=rbl+ra
```

```
end
```

```
model class stomres
```

```
parameter ro=1.0, LAI=2.0
```

```
terminal I0, rs
```

```
local s
```

```
rs=ro*(800*(1+0.5*LAI)/(1+s)/LAI)
```

```
s= I0
```

```
end
```

```
{ Bond Graph modulated longwave radiation between the sky and the  
VEGETATION CANOPY }
```

```
model class (LW) skyveg
```

```
GO = ground
```

```
end
```

```
model class (TwoPort) radexchange
```

```
submodel (skyveg) sky, veg
```

```
connect sky from A to B
```

```
connect veg from B to A
```

```
end
```

```
{ Bond Graph modulated convection (Sensible Heat) between the VEGETATION  
CANOPY and the INTERNAL ATMOSPHERE }
```

```

model class (sensible) sensveg
  terminal rb
G0= ground/rb
end

```

```

model class (TwoPort) convection
  submodel (sensveg) sensveg1
  submodel (bond) B1, B2, B3
  node n1, n2
    connect B1      from A to n1
    connect B2      from n1 to n2
    connect B3      from n1 to B
    connect sensveg1 from n2 to B
end

```

{ Bond Graph modulated convection (Latent Heat) between the VEGETATION
CANOPY and the ATMOSPHERE}

```

model class(TwoPort) latent
local G, pwsa, pwsv, pwa
terminal Ta, P, rb, rs, E
parameter a=0.61375, b=17.502, c=240.97, rhoa=1.204, lambda2= 2.5e6
{Evaporation rate*evaporisation heat}
E=lambda2*G*(pwsv-pwa)
{saturation water vapor pressures for Temperature of vegetation and
atmosphere}
pwsv=a*exp(b*(e1-273.15)/(c+(e1-273.15)))

```

```
pwsa=a*exp(b*(Ta-273.15)/(c+(Ta-273.15)))  
pwa=e2*pwsa  
E=e1*f1  
E=e2*f2  
G=0.622*rhoa/ P /(rb+rs)  
end
```

B.7 program:veg.dec

```
nsteps nstp=2000
```

```
table humidity, 1, 72 / &  
  0., 1., 2., 3., 4., &  
  5., 6., 7., 8., 9., &  
 10., 11., 12., 13., 14., &  
 15., 16., 17., 18., 19., &  
 20., 21., 22., 23., 24., &  
 25., 26., 27., 28., 29., &  
 30., 31., 32., 33., 34., &  
 35., 36., 37., 38., 39., &  
 40., 41., 42., 43., 44., &  
 45., 46., 47., 48., 49., &  
 50., 51., 52., 53., 54., &  
 55., 56., 57., 58., 59., &  
 60., 61., 62., 63., 64., &  
 65., 66., 67., 68., 69., &  
 70., 71.,           &  
 51., 49., 48., 48., 48., &  
 47., 50., 51., 53., 55., &  
 56., 56., 56., 56., 56., &  
 57., 58., 57., 56., 56., &  
 54., 53., 52., 52., 51., &  
 51., 51., 50., 50., 51., &  
 53., 54., 55., 55., 56., &  
 56., 57., 57., 57., 57., &
```

57., 57., 56., 55., 54., &
53., 52., 50., 48., 46., &
46., 46., 45., 47., 49., &
51., 53., 54., 56., 57., &
57., 58., 58., 58., 58., &
57., 57., 56., 55., 54., &
54., 52. /

table RAD, 1, 72 / &

0., 1., 2., 3., 4., &
5., 6., 7., 8., 9., &
10., 11., 12., 13., 14., &
15., 16., 17., 18., 19., &
20., 21., 22., 23., 24., &
25., 26., 27., 28., 29., &
30., 31., 32., 33., 34., &
35., 36., 37., 38., 39., &
40., 41., 42., 43., 44., &
45., 46., 47., 48., 49., &
50., 51., 52., 53., 54., &
55., 56., 57., 58., 59., &
60., 61., 62., 63., 64., &
65., 66., 67., 68., 69., &
70., 71., &
0.0, 0.0, 0.0, 0.0, 0.0, &
8.0, 60.0, 137.0, 210.0, 270.0, &
312.0, 334.0, 339.0, 328.0, 299.0, &

250.0, 184.0, 108.0, 36.0, 2.0, &
0.0, 0.0, 0.0, 0.0, 0.0, &
0.0, 0.0, 0.0, 0.0, 8.0, &
60.0, 137.0, 210.0, 270.0, 312.0, &
334.0, 339.0, 328.0, 299.0, 250.0, &
184.0, 109.0, 37.0, 2.0, 0.0, &
0.0, 0.0, 0.0, 0.0, 0.0, &
0.0, 0.0, 0.0, 8.0, 60.0, &
137.0, 210.0, 270.0, 312.0, 334.0, &
339.0, 328.0, 299.0, 251.0, 185.0, &
109.0, 37.0, 2.0, 0.0, 0.0, &
0.0, 0.0 /

B.8 program:veg.dyc

```
set Eliminate on
set AutoFileName off
set ShowFullName on
set Events on
{set CommonOn}

enter model
@veg.lib
@veg.dym
variable value c.e= 295
output equations
outfile veg.eql
    output equations

outfile
partition

outfile veg.seq
    output sorted equations
outfile veg.sleq
    output solved equations

simulation StopTime=24, algorithm=2, Interval=0.1
language ACSL
```

```
outfile veg.csl
```

```
  output model
```

```
outfile veg.cmd
```

```
  output experiment
```

```
quit
```